Online Appendix — Not for Publication

Navigating the Waves of Global Shipping: Drivers and Aggregate Implications[1]

Jason Dunn (Boston University), Fernando Leibovici (FRB St. Louis)

April 2026

[1]Correspondence address: fleibovici@gmail.com. The views expressed herein are those of the individual authors and do not necessarily reflect official positions of the Federal Reserve Bank of St. Louis, the Federal Reserve System, or the Board of Governors.

Part I

Data

1 Data Documentation

The following table documents all data series used in the paper and appendix, and details regarding any transformations made to the raw data.

Table 1: Data Sources

Section	Figure/Table	Data Used	Source	Period	Transformation/Processing Notes
1	Figure 1	Drewry World Container Index	Drewry	2006Q1-2019Q4	Deflated by aggregate CPI, ln, HP filter (λ=1600), cyclical component
1	Figure 2, Panel A	Household final consumption: durables, semidurables, non-durables	OECDstat	2015Q1-2024Q4	ln of variable, normalize by subtracting 2019Q4 and adding 1, weighted avg. across countries
1	Figure 2, Panel B	Imports of goods and services	OECDstat	2015Q1-2024Q4	ln of variable, normalize by subtracting 2019Q4 and adding 1, weighted avg. across countries
1	Figure 2, Panel C	Drewry World Container Index	Drewry	2015Q1-2024Q4	level (USD/40ft container)
2	Figure 3, Panel A	Total Containerships Fleet Development	Clarksons	1996-2024	level (TEU million, number)
2	Figure 3, Panel B	Total Containerships - Idle (TEU); Load factor; Effective Utilization	Clarksons; AIS	2014-2024	level (Fleet - Idle) / Fleet; level (draught / max_draught); level (Non-Idle * Load factor)
2	Figure 3, Panel C	Containerships Contracting; Clarksons Charter Market Basket Earnings; Drewry World Container Index	Clarksons	1996-2024	level (Contracting); ln Annual change earnings (1996-2006) or costs (2007-2024)
2	Figure 3, Panel D	Containership Contract and Build Dates	Clarksons	April 2024 Snapshot	level (time in quarters)
2	Figure 3, Panel E	Industrial production; Total Containerships Fleet Development	Dallas Fed; Clarksons	1996-2024	ln Annual change
2	Figure 3, Panel F	Industrial production; Total Containerships Fleet Development; Clarksons Charter Market Basket Earnings; Drewry World Container Index	Dallas Fed; Clarksons; Drewry	1996-2024	ln (Annual change IP / Annual change Fleet); ln Annual change earnings (1996-2006) or costs (2007-2024)
5	Table 1, Intermediate Share in gross output: Tradables	Intermediate Consumption in Goods; Value Added at Factor Prices in Goods	OECDstat	1996-2019	t_totalinputs / (t_valueadded_factorprices + totalinputs)
5	Table 1, Intermediate Share in gross output: Non-Tradables	Intermediate Consumption in Services; Value Added at Factor Prices in Services	OECDstat	1996-2019	nt_totalinputs / (nt_valueadded_factorprices + nt_totalinputs)
5	Table 1, Share of Tradables: Consumption Goods	Household final consumption: durables, semidurables, non-durables; Total economy final consumption expenditure	OECDstat	1996-2019	tradconsumption / aggconsumption
5	Table 1, Share of Tradables: Capital Goods	Capital detail: Investment data by assets	PWT	1996-2019	(Machines + TransportEq + Other) / (Structures + Machines + TransportEq + Other)
5	Table 1, Shipping depreciation rate	Containership Contracting; Total Containerships Fleet Development	Clarksons	1996-2019	delta_y = (ShipInv / Fleet) - ln(Annual Fleet Growth); Convert to Quarterly: delta_q = 1 - (1 - delta_y)^(1/4)
5	Table 1, Shipping production lag	Containership Contract and Build Dates	Clarksons	April 2024 Snapshot	approximate lower bound for time to build
5	Table 2, Share of agg. Imports: Capital	BEC SNA Capital class imports	Comtrade	1996-2019	(cifvalue capital imports) / (cifvalue total imports)
5	Table 2, Share of agg. Imports: Intermediates	BEC SNA Intermediate class imports	Comtrade	1996-2019	(cifvalue intermediate imports) / (cifvalue total imports)
5	Table 2, Agg. Tradables: Imports / Absorption	Imports of goods; Exports of goods; Gross domestic product	OECDstat	1996-2019	goodsimports / (rGDP - goodsexports + goodsimports)
5	Table 2, Shipping Costs / Imports	World transport expenditure and FOB values	UNCTAD	2016-2019	transport_expenditure_us_value / fob_value_us_value
5	Table 2, Shipping Utilization	Total Containerships - Idle (TEU); Load factor	Clarksons; AIS	2015-2019	level (Fleet - Idle) / Fleet * level (draught / max_draught)
5	Table 3, Std. dev. Real GDP	Gross domestic product	OECDstat	1996Q1-2019Q4	ln, HP filter (λ=1600), cyclical component, std. dev., weighted avg. across countries
5	Table 3, Std. dev. Investment / Std. dev. Real GDP	Gross capital formation	OECDstat	1996Q1-2019Q4	ln, HP filter (λ=1600), cyclical component, std. dev., weighted avg. across countries

Table 1: Data Sources

Section	Figure/Table	Data Used	Source	Period	Transformation/Processing Notes
5	Table 3, Std. dev. Imports / Std. dev. Tradable output	Imports of goods and services; Household final consumption: durables, semidurables, non-durables; Gross capital formation of machinery	OECDstat	1996Q1-2019Q4	ln, HP filter (λ=1600), cyclical component, std. dev., weighted avg. across countries
5	Table 4, Std. dev. GDP	Gross domestic product	OECDstat	1996Q1-2019Q4	ln, HP filter (λ=1600), cyclical component, std. dev., weighted avg. across countries
5	Table 4, Std. dev. Net Exports / GDP	Exports of goods and services; Imports of goods and services	OECDstat	1996Q1-2019Q4	HP filter (λ=1600), cyclical component, std. dev., weighted avg. across countries
5	Table 4, Std. dev. Consumption / Std. dev. Real GDP	Final consumption expenditure	OECDstat	1996Q1-2019Q4	ln, HP filter (λ=1600), cyclical component, std. dev., weighted avg. across countries
5	Table 4, Std. dev. Investment / Std. dev. Real GDP	Gross capital formation	OECDstat	1996Q1-2019Q4	ln, HP filter (λ=1600), cyclical component, std. dev., weighted avg. across countries
5	Table 4, Std. dev. Labor / Std. dev. Real GDP	Total employment	OECDstat	1996Q1-2019Q4	ln, HP filter (λ=1600), cyclical component, std. dev., weighted avg. across countries
5	Table 4, Std. dev. Tradables-Nontradables Price / Std. dev. Real GDP	Goods CPI; Services CPI	OECDstat	1996Q1-2019Q4	ln, HP filter (λ=1600), cyclical component, std. dev., weighted avg. across countries
5	Table 4, Std. dev. Terms of trade / Std. dev. Real GDP	Terms of trade, goods and services	OECDstat	1996Q1-2019Q4	ln, HP filter (λ=1600), cyclical component, std. dev., weighted avg. across countries
5	Table 4, Std. dev. Real exchange rate / Std. dev. Real GDP	Real effective exchange rate, constant trade weights	OECDstat	1996Q1-2019Q4	ln, HP filter (λ=1600), cyclical component, std. dev., weighted avg. across countries
5	Table 4, Std. dev. Shipping Costs / Std. dev. Real GDP	Drewry World Container Index	Drewry	2006Q1-2019Q4	ln, HP filter (λ=1600), cyclical component, std. dev.
5	Table 4, Std. dev. Shipping Capacity / Std. dev. Real GDP	Total Containerships Fleet Development (TEU)	Clarksons	1996Q1-2019Q4	ln, HP filter (λ=1600), cyclical component, std. dev.
5	Table 4, Std. dev. Shipping investment rate	Total Containerships Fleet Development (TEU)	Clarksons	1996Q1-2019Q4	standard deviation of the quarterly growth rate of fleet TEU
6	Figure 5, Panel 3	Household final consumption: durables, semidurables, non-durables	OECDstat	2020Q3-2024Q4	ln deviation from 2015Q1-2019Q4 trend
6	Figure 5, Panel 6	Gross capital formation: machines	OECDstat	2020Q3-2024Q4	ln deviation from 2015Q1-2019Q4 trend
6	Figure 5, Panel 9	Ocean Timeliness Index	Flexport	2020Q3-2024Q4	ln(2020Q1-2020Q3 / Quarterly Avg time: de-seasonalized and net cargo dwell)
6	Figure 5, Panel 12	Gross domestic product	OECDstat	2020Q3-2024Q4	ln deviation from 2015Q1-2019Q4 trend
6	Figure 6, Panel 1	Gross capital formation	OECDstat	2020Q3-2024Q4	ln deviation from 2015Q1-2019Q4 trend
6	Figure 6, Panel 2	Final consumption expenditure	OECDstat	2020Q3-2024Q4	ln deviation from 2015Q1-2019Q4 trend
6	Figure 6, Panel 3	Total employment	OECDstat	2020Q3-2024Q4	ln deviation from 2015Q1-2019Q4 trend
6	Figure 6, Panel 4	Goods CPI; Services CPI	OECDstat	2020Q3-2024Q4	ln deviation from 2015Q1-2019Q4 trend
6	Figure 6, Panel 5	Household final consumption: durables, semidurables, non-durables; Gross capital formation: machines	OECDstat	2020Q3-2024Q4	ln deviation from 2015Q1-2019Q4 trend
6	Figure 6, Panel 6	Aggregate final consumption and gross capital formation net of tradable consumption and tradable investment	OECDstat	2020Q3-2024Q4	ln deviation from 2015Q1-2019Q4 trend
6	Figure 7, Panel 1	Drewry World Container Index	Drewry	2020Q3-2024Q4	ln deviation from 2015Q1-2019Q4 trend
6	Figure 7, Panel 2	Containerships Contracting; Total Containerships Fleet Development (TEU)	Clarksons	2020Q3-2024Q4	level deviation from 2015Q1-2019Q4 average
6	Figure 7, Panel 4	Monthly Global Seaborne Container Trade Index; Volume Index	Clarksons	2020Q3-2024Q4	Disagg. annual trade by monthly index, seas. adj., ln deviation from 2015Q1-2019Q4 trend

Table 1: Data Sources

Section	Figure/Table	Data Used	Source	Period	Transformation/Processing Notes
A	Section 2 (COVID-19), Figure 1, Panel 1	Monthly Global Seaborne Container Trade Index; World Seaborne Container Trade	Clarksons	2020Q3-2024Q4	Disagg. annual trade by monthly index, seas. adj. by quarterly dummies, ln deviation from 2015Q1-2019Q4 trend
A	Section 2 (COVID-19), Figure 1, Panel 2	China to US West Coast Voyage Duration; Port-to-Port Transit Time; Ocean Timeliness	Clarksons; Freightos; Flexport	2020Q3-2024Q4	de-seasonalized level (days) (net cargo dwell for Flexport)
A	Section 2 (COVID-19), Figure 1, Panel 3	Port Congestion Index; Containerships in Port	Clarksons	2020Q3-2024Q4	% of fleet in port, 7 day moving average
A	Section 3 (Spot v. effective), Figure 2	Port-level shipping freight rates; Container trade charges/value/weight	Drewry; USTrade-Census	2015Q1-2024Q4	ln (Quarterly average / 2020Q1)
A	Section 4a (Shares), Tables 2/3	Trade value and weight by HS commodity	USTrade-Census	2003-2024	average by mode of transport
A	Section 4a (Shares), Table 3, Col 4	World Seaborne Container/Dry Bulk/Total Trade	Clarksons	2003-2024	average by mode of transport
A	Section 4b (Bulk Long Run), Figure 3, Panel A/B	Total Containership/Bulk Carrier Fleet Development; Idle fleet	Clarksons	1996-2024	level
A	Section 4b (Bulk Long Run), Figure 3, Panel C/D	Containership/Bulker Contracting; Average weighted earnings	Clarksons	1996-2024	level (Contracting); ln Annual change (Earnings)
A	Section 4b (Bulk Long Run), Figure 3, Panel E	Industrial Production; Fleet Development; Average Earnings	Dallas Fed; Clarksons	1996-2024	ln (Annual change IP / Annual change Fleet); ln Annual change earnings
A	Section 4b (Bulk Long Run), Figure 3, Panel F	Industrial Production; Total Bulkcarrier Fleet Development; Average weighted earnings all bulkers	Dallas Fed; Clarksons	1996-2024	ln (Annual change IP / Annual change Fleet); ln Annual change earnings
A	Section 4c (Bulk COVID), Figure 4, Panel 1	Baltic Exchange Dry Index; Drewry World Container Index	Clarksons; Drewry	2006Q1-2024Q4	ln change from 2010-2019 mean
A	Section 4c (Bulk COVID), Figure 4, Panel 2	Monthly Global Seaborne Container/Dry Bulk Trade Index and Volume	Clarksons	2015Q1-2024Q4	Disagg. annual trade by monthly index, seas. adj., ln deviation from 2015Q1-2019Q4 trend
A	Section 5 (Time to Build), Figure 5, Panel A	Containership Contract and Build Dates	Clarksons	April 2024 Snapshot	TEU share by size
A	Section 5 (Time to Build), Figure 5, Panel B	Containership Contract and Build Dates	Clarksons	April 2024 Snapshot	TEU share by period
A	Section 5 (Time to Build), Figure 6	Containership Contract and Build Dates	Clarksons	April 2024 Snapshot	Total TEU, mean and median build time by period
A	Section 9 (Business cycle dynamics), Table 8	See Paper Table 4 description	OECDstat; Drewry; Clarksons	1996Q1-2019Q4	ln, HP filter (λ=1600), cyclical component, correlation with global sum, weighted avg. across countries
A	Section 10 (COVID-19), Figure 11, Panel 1	Firm closing stock price	Yahoo Finance	2020Q3-2024Q4	ln deviation from 2015Q1-2019Q4 trend
A	Section 10 (COVID-19), Figure 11, Panel 2	Firm gross profits; Firm revenue	Yahoo Finance	2020Q3-2024Q4	absolute deviation from 2015Q1-2019Q4 trend
A	Section 10 (COVID-19), Figure 11, Panel 3	Firm EBIT; Firm revenue	Yahoo Finance	2020Q3-2024Q4	absolute deviation from 2015Q1-2019Q4 trend

Figure 1: Shipping disruptions during COVID-19

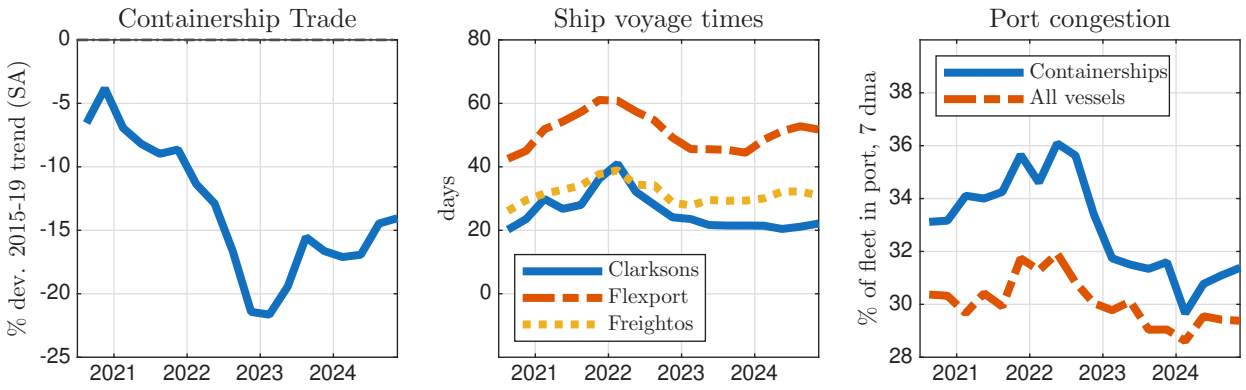

Note: Data from Clarkson's *Shipping Intelligence Network*, Flexport, and Freightos. Containership trade is measured using Clarksons data on total containership trade, expressed in TEUs, as changes relative to the 2015–2019 trend of the seasonally-adjusted series. Clarksons China to US West Coast: containership voyage average duration derived from AIS vessel movements data. Flexport's Ocean Timeliness Indicator measures freight shipping time from when cargo is ready to leave the exporter to when it is collected from its destination port, averaged across China–Northern Europe, China–US West Coast, and China–US East Coast routes. Freightos: average ship trip length into all US ports. Clarksons Port Congestion Index: proportion of vessels (in TEU) in a defined port or anchorage location, based on the vessel's closest to midday AIS signal, 7-day moving average.

2 Shipping disruptions during COVID-19

The COVID-19 pandemic caused significant disruptions to global shipping, leading to a contraction in effective shipping capacity. This section provides additional context on the shipping efficiency shock modeled in our quantitative exercise. We present both empirical evidence from key shipping indicators and anecdotal reports from major ports to highlight the nature and extent of these disruptions.

2.1 Quantitative evidence

Figure 1 presents three key indicators of shipping disruptions during the pandemic: containership trade, voyage times, and port congestion.

The left panel shows containership trade, calculated as the log-deviation from the 2015-2019 trend of the seasonally-adjusted series. This measure serves as a coarse proxy for the effective use of global shipping capacity. The observed decline in trade during COVID-19, despite higher demand for tradable goods, reflects widespread reduced effective shipping capacity caused by port congestion, shipping delays, and labor shortages.

The middle panel shows average voyage times across major shipping routes, illustrating a significant increase during the pandemic. Ships were delayed at ports due to health restrictions, crew shortages, and longer turnaround times, reducing the availability of shipping services and contributing to the decline in effective capacity. The Flexport series is used in the paper to back out the productivity shock $\bar{g}$ to shipping efficiency in our baseline results.

The right panel displays port congestion data for containerships and all vessel types. Ports around the world experienced unprecedented delays, with ships waiting offshore for extended periods before being processed. This congestion further constrained the shipping industry's ability to meet rising demand and

drove up shipping costs.

2.2 Anecdotal evidence of port restrictions and crew shortages

Anecdotal evidence from major ports provides further insight into the specific disruptions that reduced shipping capacity. For example, Chinese ports implemented stringent quarantine measures for incoming vessels. The port of Fuzhou, for instance, imposed a requirement for ships arriving from certain countries to wait up to 14 days before docking, significantly delaying ship processing.[2] In the United States, the ports of Los Angeles and Long Beach faced significant operational challenges due to labor shortages and increased cargo volumes. COVID-19 infections among dockworkers led to slowdowns in operations, with dozens of cargo ships anchored offshore and waiting to be offloaded.[3]

Additionally, the pandemic caused a global crew change crisis, with an estimated 400,000 seafarers stranded on vessels due to international travel restrictions. In China, for example, returning seafarers were subjected to mandatory quarantine periods of up to seven weeks, further delaying shipping operations.[4]

The combination of quantitative indicators and anecdotal evidence provides broad support for our interpretation of the shipping efficiency shock modeled in our quantitative exercise. The disruptions observed during the pandemic played a crucial role in driving the supply chain bottlenecks and trade slowdowns that significantly impacted global shipping capacity.

3 Shipping costs: Spot vs. effective rates

In this section, we contrast the shipping cost measure that we use throughout the paper relative to other methods of measuring shipping costs. The benchmark series we use for comparison and analysis is the Global Drewry average spot rate for 40-foot containers. It is important to note that while spot rates are among the most cited measures of shipping costs, they may not be representative of overall effective shipping costs given that some carriers engage in longer-term contracts that do not adjust immediately in response to shocks.

To evaluate whether spot rates reflect effective shipping costs, we compare the Drewry spot rates to U.S. trade cost data from the U.S. Census. Specifically, Figure 2 shows four series: the Drewry container index for U.S. ports, the U.S. Census measure of freight and insurance charges per kilogram of trade, and the ratio of CIF (cost, insurance, and freight) to FOB (free on board) values, with and without insurance.[5] Critically, these alternative measures of shipping costs capture the effective shipping cost paid, combining both spot rates and long-term contracts. Each series is expressed as a log change relative to 2020Q1. We

[2]TTNews, "Chinese Port Restricts Ships From Virus-Hit Nations for 14 Days," available at `https://www.ttnews.com/articles/chinese-port-restricts-ships-virus-hit-nations-14-days`

[3]NewsNation, "COVID-19 Infections Among Hundreds of Workers Lead to Cargo Ship Traffic Jam," available at `https://www.newsnationnow.com/business/covid-19-infections-among-hundreds-of-workers-lead-to-cargo-ship-traffic-jam`

[4]Supply Chain Digital, "7-Week Quarantine for Ship Crew in China Hits Supply Chain," available at `https://supplychaindigital.com/logistics/7-week-quarantine-ship-crew-china-hit-supply-chain`

[5]To calculate the CIF/FOB rate without insurance, we remove 0.5% from the CIF before calculating percent changes. The 0.5% insurance estimate is taken from Freightos: `https://www.freightos.com/freight-resources/freight-insurance`.

Figure 2: Shipping costs, spot vs. effective rates

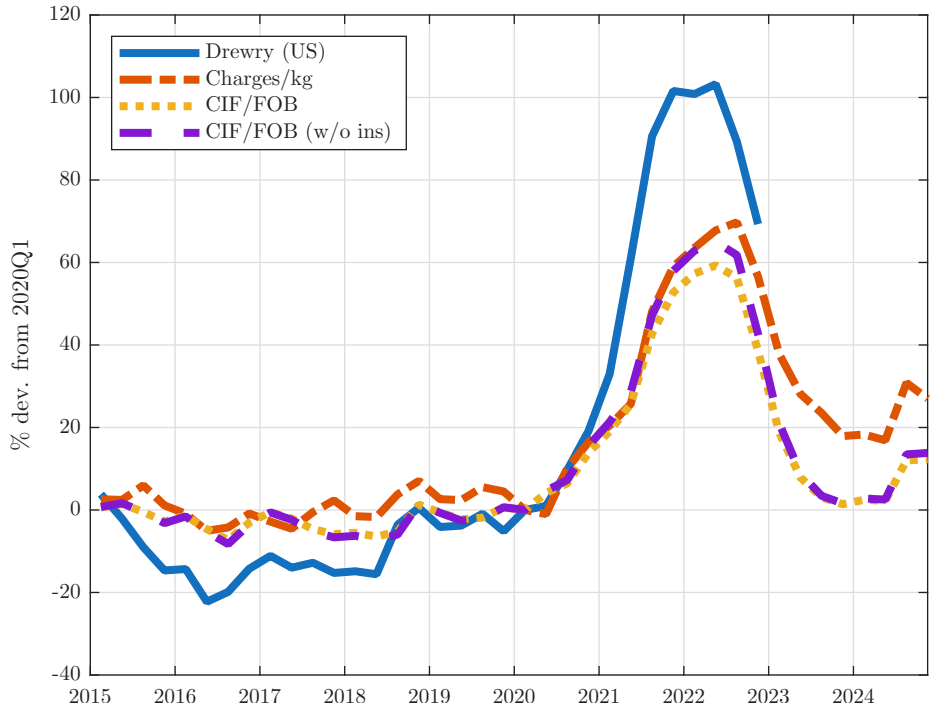

Data from Drewry Supply Chain Advisors and US Trade Census.

restrict attention to U.S. imports given that data limitations prevent us from computing these variables systematically across countries — this is why we focus on global spot rates in the paper.

The comparison suggests that the effective shipping costs measured using U.S. Census data and the CIF/FOB ratio exhibit trends similar to the Drewry spot rates during the pandemic, albeit with less pronounced fluctuations. The freight and insurance charges per kilogram and the CIF/FOB ratio (with and without insurance) both increased significantly during the pandemic, but their increases were milder in magnitude than spot rates. This difference is consistent with the notion that spot rates are more sensitive to immediate supply and demand shocks, whereas aggregate shipping costs capture a broader set of shipping arrangements, including longer-term contracts.

Overall, the comparison indicates that the Drewry spot rates capture the direction and timing of changes in shipping costs observed in aggregate trade data. While the lack of data availability on effective shipping costs across countries prevents us from comparing spot vs. effective rates across countries, the findings reported in this section suggest the spot rates used in our model reflect broader shipping cost trends, making them a suitable proxy for the purpose of this study.

Table 2: Total trade shares

	Value share		Volume share	
Mode	**US**	**Global**	**US**	**Global**
Sea	43.1%	30.5%	99.4%	$> 99\%$
Air	26.6%	14.1%	0.6%	$< 1\%$
Land	30.3%	42.4%	-	-
Other	-	12.9%	-	-

Columns 1 and 3 are 2003 - 2024 averages from the US Trade Census for both exports and imports. Column 2 is the 2003 - 2024 average from a sample of 46 countries from Comtrade. Column 4 is a 2021 value reported in Boeing World Air Cargo Forecast 2022 - 2041. In columns where the "Land" and/or "Other" categories are omitted, it is because those categories are not included in that data.

4 Containers and global shipping

Understanding the role of container shipping in global trade is crucial to assessing the broader impact of shipping disruptions on economic fluctuations. While the paper focuses on container shipping, this section provides additional context by examining the value and volume of goods transported by different shipping modes, comparing industry dynamics across container and bulk shipping, and analyzing trade fluctuations following the COVID-19 pandemic. The evidence presented here shows that container shipping accounts for a significant share of global trade value, exhibits dynamics similar to other important seaborne shipping markets, and experienced trade fluctuations comparable to bulk shipping during COVID-19.

4.1 Containers: Value and volume of goods shipped

To assess the significance of container shipping within global trade, it is useful to examine the breakdown of trade by different shipping modes. Tables 2 and 3 present the distribution of trade shares across sea, air, and land, both globally and for the United States. These tables highlight the dominant role of maritime shipping in international trade and the substantial contribution of containerships.

Table 2 shows that sea shipping accounts for a significant share of global trade, both in value and volume. Globally, around 30.5% of trade value is transported by sea, while in the U.S., sea shipping represents 43.1% of trade value. In terms of volume, sea shipping dominates air: relative to air shipping, more than 99% of the volume of goods transported in the U.S. and globally are moved by sea.[6] Air freight trade values are higher given the prevalence of high-value goods.

These patterns highlight the limited scope for mitigating COVID-19-related shipping disruptions through a reallocation from sea shipments to air or land transport. First, air shipping capacity (in terms of volume) is minimal compared to sea shipping capacity. Second, land-based reallocation is only feasible for shipments between geographically proximate and connected locations.

Table 3 provides a breakdown of sea transport by shipping type. Containerships account for a substantial portion of sea trade by value, representing 55.4% and 48.8% of U.S. and global sea trade value,

[6]Data limitations prevent us from comparing trade volumes relative to land.

Table 3: Sea trade shares

Mode	Value share		Volume share	
	US	Global	US	Global
Containerships	55.4%	48.8%	12.6%	14.0%
Dry Bulk	8.2%	11.4%	34.3%	43.1%
Other	36.4%	39.7%	53.1%	42.9%

Columns 1 and 3 correspond to those in Table 2. To classify the goods shipped between containerships and dry bulk, we consider the following HS commodities as containership goods: 7-9, 16, 19-22, 39-40, 50-63, 68-70, 73-74, 76, 78-79, 84-88, 90-91, 94-96. We consider the following commodities as dry bulk goods: 10, 12, 23, 25-26, 28, 31, 44, 47-48, 2701-2704, 2713. Column 4 is the 2003 - 2024 average from Clarkson's *Shipping Intelligence Network*.

respectively. In terms of volume, containerships represent about 12.6% of U.S. sea shipping volume and approximately 14% globally. Bulk shipping accounts for most of the remaining sea trade volume.

These figures underscore that container shipping accounts for a significant portion of global trade value and plays a key role in maritime transport worldwide, making it central to understanding global shipping dynamics.

4.2 Industry dynamics: Containers vs. bulk

Given that container and bulk shipping together account for the majority of sea trade, it is useful to examine whether the dynamics observed in the containership sector extend to bulk shipping as well. Figure 3 shows these subsectors exhibit similar patterns across fleet growth, capacity utilization, new orders relative to earnings, and the relationship between earnings and excess demand.[7] The observed similarities suggest that the key economic forces driving shipping dynamics are common across shipping modes and not unique to containerships.

The top left panel of Figure 3 shows that fleet sizes for both container and bulk shipping have grown steadily over time, reflecting consistent investment in shipping capacity across both markets. The top right panel illustrates extensive capacity utilization rates for these subsectors, which have remained high and stable, indicating a persistent balance between supply and demand in both the containership and bulk shipping markets.

The middle panels of Figure 3 show new orders and average earnings for both subsectors. In both cases, we observe a positive relationship between earnings and new orders, indicating that periods of higher earnings are also ones featuring increases in new ship orders. This similarity suggests that investment decisions are driven by comparable incentives across both subsectors.

The bottom panels of Figure 3 illustrate the relation between earnings and excess demand for both container and bulk shipping. The positive correlation observed in both markets (0.70 for bulk and 0.66 for containerships) further demonstrates that pricing and investment dynamics are driven by similar economic

[7]For this comparison, we use Clarkson's earnings series for both containerships and bulk shipping in order to maintain comparability across sectors. This differs from the main paper's containership series, which combines Clarkson's containership earnings series with the Drewry World Container Index in later years.

forces, regardless of subsector.

The left panel of Figure 4 shows that spot rates for containers (Drewry World Container Index) and dry bulk (Baltic Dry Index) have followed similar trends over the past 20 years. However, the Great Recession had a more pronounced impact on dry bulk rates, while the effects of COVID-19 were slightly more significant for containerships.

The dynamics of global trade following the COVID-19 pandemic further support the relevance of our focus on container shipping. The right panel of Figure 4 compares trade dynamics for containers and dry bulk shipping, showing the detrended and seasonally-adjusted world trade volume relative to 2020Q1 for both segments. We observe that both container and dry bulk shipping experienced similar trends in the aftermath of the pandemic.

These similarities are particularly noteworthy given the differences in market structure between the two subsectors. The containership sector is dominated by a few large firms, with the top 10 companies controlling approximately 80% of the market. These firms often operate through strategic alliances to coordinate capacity and routes. In contrast, bulk shipping is much more fragmented and competitive, with a large number of smaller operators. The bulk shipping market, as studied by Kalouptsidi (2014) and Brancaccio et al. (2020), is generally considered a benchmark for competitive behavior in shipping markets.

Despite these differences in market structure, the observed dynamics across both subsectors are remarkably similar, including fleet growth, capacity utilization, investment responses to earnings, and spot rates. This suggests that the shipping dynamics we observe are unlikely to be driven primarily by differences in market structure. Instead, they appear to reflect broader economic forces that are common across different types of sea shipping.

Figure 3: Shipping industry dynamics, containers vs. dry bulk

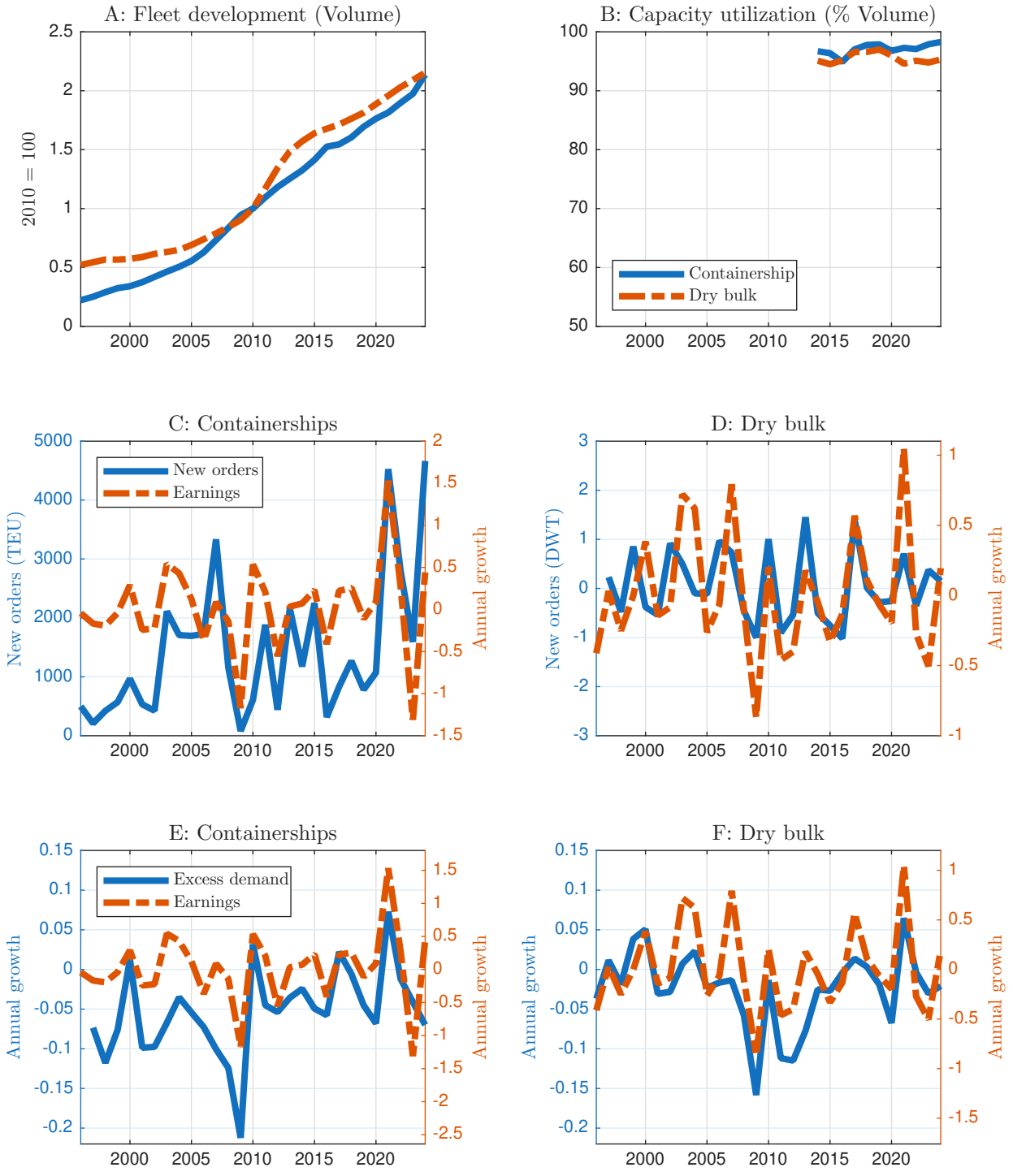

Note: Data from Clarkson's *Shipping Intelligence Network* and *IMF*.

Figure 4: Shipping prices and trade, containers vs. dry bulk

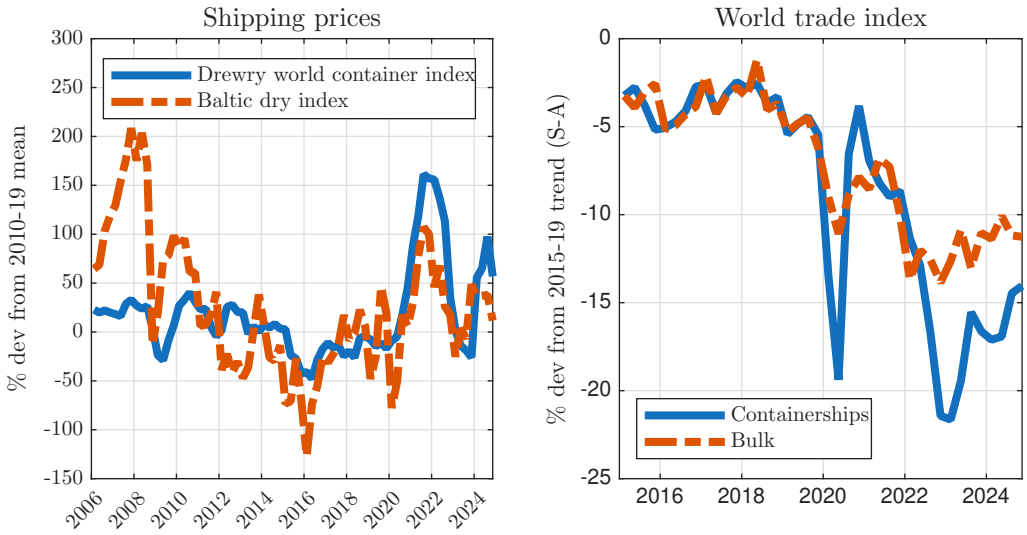

Note: Data from Clarkson's *Shipping Intelligence Network* and Drewry Supply Chain Advisors.

5 Containership time-to-build

Understanding the time it takes to build new containerships is essential for assessing the dynamics of shipping capacity. In this section, we examine how the time-to-build varies both by ship size and across different time periods.

The left panel of Figure 5 presents the distribution of time-to-build by ship size, measured in quarters, using data from Clarkson's *Shipping Intelligence Network*. The figure shows that construction times remain relatively uniform across different ship sizes, suggesting that production lags are not significantly affected by vessel size. This indicates that shipyards can maintain similar timelines regardless of the ships' dimensions.

Next, we examine how time-to-build varies over time. The right panel of Figure 5 presents the distribution of time-to-build by time period. These distributions exhibit more variation than those across ship size, suggesting there may be some factors that vary by time period and influence time to build.

To further explore this, Figure 6 illustrates that the relationship between time period and time-to-build may be driven by demand for new ships. The scatterplot shows the relationship between the size of ship orders (in TEUs) and the time-to-build. The left panel presents the mean time-to-build, while the right panel presents the median time-to-build, with each point representing a two-year period from 2000 to 2019. Both panels indicate a positive relationship between the volume of orders and the time-to-build. This indicates that time-to-build extends during periods of heightened ordering activity, consistent with the idea that increased demand strains shipyard capacity and leads to longer production timelines.

Figure 5: Containership time-to-build by ship size and time period

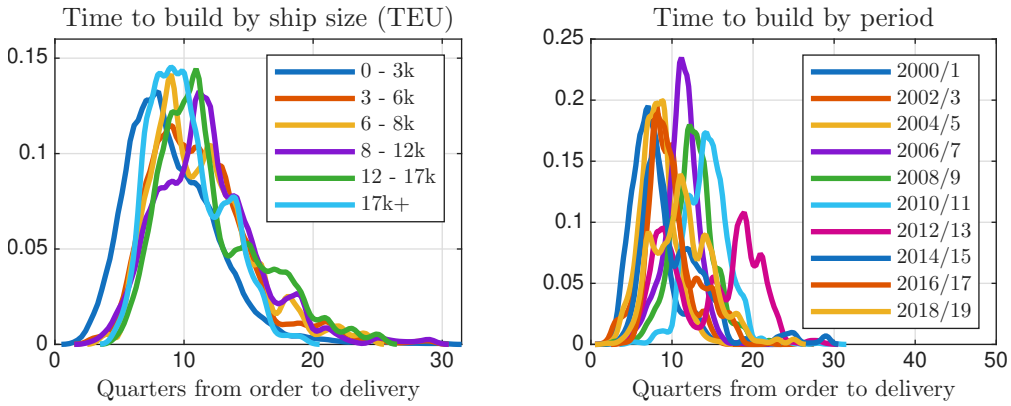

Note: Data from Clarkson's *Shipping Intelligence Network*.

Figure 6: Containership time-to-build, amount ordered vs. build time

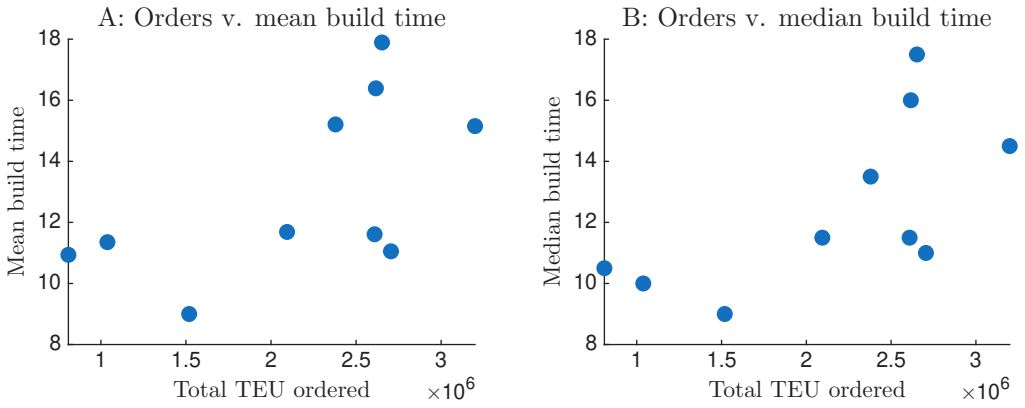

Note: Data from Clarkson's *Shipping Intelligence Network*. Each point represents a two year period from 2000 - 2019.

Part II

Model and Quantitative Results

6 Model

6.1 Equilibrium

An equilibrium is a sequence of prices and allocations such that, given initial conditions and stochastic processes, all agents optimize and all markets clear in every period.

Prices. An equilibrium features sequences of prices

$$\{p_t^c, p_t^m, p_t^k, p_t^{c*}, p_t^{m*}, p_t^{k*}, p_{Tt}, p_{Tt}^*, p_{Nt}, p_{Nt}^*, h_t, w_t, w_t^*, r_{Kt}, r_{Kt}^*, r_t, r_t^*\}_{t=0}^{\infty},$$

where $p_t^c \equiv 1$ is the numeraire.

Allocations. An equilibrium also features sequences of allocations

$$\{c_t, n_t, i_t, k_{t+1}, b_{t+1}\}_{t=0}^{\infty}, \qquad \{c_t^*, n_t^*, i_t^*, k_{t+1}^*, b_{t+1}^*\}_{t=0}^{\infty},$$

firm-level input and output choices for all production sectors, bundle quantities

$$\{y_t^\ell, q_{Tt}^{\ell h}, q_{Tt}^{\ell f}, q_{Nt}^\ell\}_{\ell\in\{m,c,k\},t\geq 0}, \qquad \{y_t^{\ell *}, q_{Tt}^{\ell f *}, q_{Tt}^{\ell h *}, q_{Nt}^{\ell *}\}_{\ell\in\{m,c,k\},t\geq 0},$$

and shipping choices $\{g_{t+J}, \upsilon_t, i_{Gt}\}_{t=0}^{\infty}$.

Profits. Profits earned by the household are given by: $\Pi_t = \sum_{\ell\in\{c,k,m\}} \pi_t^\ell + \sum_{j\in\{T,N\}} \pi_{jt}$.

Market clearing. In every period t, the following market-clearing conditions hold:

- *Labor markets:*

$$n_t = \sum_{j\in\{T,N\}} n_{jt}, \qquad n_t^* = \sum_{j\in\{T,N\}} n_{jt}^*$$

- *Capital markets:*

$$k_t = \sum_{j\in\{T,N\}} k_{jt}, \qquad k_t^* = \sum_{j\in\{T,N\}} k_{jt}^*$$

- *Non-tradable goods markets:*

$$y_{Nt} = \sum_{\ell\in\{m,c,k\}} q_{Nt}^\ell, \qquad y_{Nt}^* = \sum_{\ell\in\{m,c,k\}} q_{Nt}^{\ell *}$$

- *Tradable varieties markets:*

$$y_{Tt} = \sum_{\ell\in\{m,c,k\}} \left(q_{Tt}^{\ell h} + \tau q_{Tt}^{\ell h *}\right), \qquad y_{Tt}^* = \sum_{\ell\in\{m,c,k\}} \left(q_{Tt}^{\ell f *} + \tau q_{Tt}^{\ell f}\right)$$

- *Shipping services market:*

$$\sum_{\ell\in\{m,c,k\}} \left(q_{Tt}^{\ell f} + q_{Tt}^{\ell h *}\right) = \upsilon_t \overline{g}\, g_t$$

- *Goods markets for bundles:*

$$y_t^c = c_t + \frac{\Phi_b}{2} b_{t+1}^2, \qquad y_t^{c*} = c_t^* + \frac{\Phi_b}{2} b_{t+1}^{*2}$$

$$y_t^m = \sum_{j \in \{T,N\}} m_{jt}, \qquad y_t^{m*} = \sum_{j \in \{T,N\}} m_{jt}^*$$

$$y_t^k = i_t + \frac{\Phi_k}{2} \left(i_t - \delta \overline{k}\right)^2 + \psi \left[i_{Gt} + C(\upsilon_t) g_t\right]$$

$$y_t^{k*} = i_t^* + \frac{\Phi_k}{2} \left(i_t^* - \delta \overline{k}^*\right)^2 + (1 - \psi) \left[i_{Gt} + C(\upsilon_t) g_t\right]$$

- *International financial market:*

$$b_{t+1} + b_{t+1}^* = 0, \qquad r_t = r_t^*$$

(Under financial autarky, $b_{t+1} = b_{t+1}^* = 0$.)

Definition. An equilibrium is a set of prices and allocations satisfying household's optimality conditions, firm's optimality conditions in all production stages, the global shipping firm's optimality conditions, and all market-clearing conditions, given initial conditions and the exogenous stochastic processes.

6.2 Measurement

Real GDP Following Kehoe and Ruhl (2008), we measure real GDP on the production side by valuing all quantities at steady–state prices. Fixing prices in this way ensures that changes in real GDP reflect variations in quantities—such as production, trade, and shipping activity—rather than movements in relative prices or the terms of trade.

Let p_T^{ss}, p_N^{ss}, and p_m^{ss} denote the steady–state prices of tradable goods, non–tradables, and the intermediate inputs, respectively. Let y_{Tt} and y_{Nt} denote gross output in the tradable and non–tradable sectors, and let m_{Tt} and m_{Nt} denote intermediate inputs used by each sector. Then,

$$Y_t^{\text{real}} = \underbrace{p_T^{ss}\, y_{Tt}}_{\text{tradable output}} + \underbrace{p_N^{ss}\, y_{Nt}}_{\text{nontradable output}} - \underbrace{p_m^{ss}(m_{Tt} + m_{Nt})}_{\text{intermediate inputs}}$$

$$+ \underbrace{\psi\, h^{ss} \left(\upsilon_t\, \overline{g}\, g_t\right)}_{\text{value of shipping services}} - \underbrace{\psi\, p_G^{ss}\, C(\upsilon_t)\, g_t}_{\text{shipping utilization cost}} .$$

The last two terms capture the contribution of the global shipping firm. The first term reflects the value of shipping services produced, equal to the effective quantity of shipping services $\upsilon_t \overline{g} g_t$ valued at the steady–state price h^{ss}, multiplied by the home ownership share ψ. The second term subtracts utilization costs, which represent real resource costs required to operate the installed shipping capacity. Hence, net value added from shipping in home GDP equals the home ownership share of the value of shipping services net of utilization costs.

Net exports and Imports We measure the nominal trade balance (net exports) using trade flows measured Free on Board (FOB). The value of trade represents the gross units produced and dispatched

from the exporting country's dock, but excludes shipping costs h_t. Valuing exports at the price of home tradable varieties p_{Tt} and imports at the price of foreign tradable varieties p^*_{Tt}, net exports are given by:

$$\text{Net exports}_t = \sum_{\ell \in \{m,c,k\}} \left(\tau \, p_{Tt} \, q^{\ell h *}_{Tt} \right) - \sum_{\ell \in \{m,c,k\}} \left(\tau \, p^*_{Tt} \, q^{\ell f}_{Tt} \right).$$

Similarly, the volume of real imports is evaluated using steady-state foreign tradable prices p^{ss*}_T to remove valuation effects from price:

$$\text{Real imports}_t = \sum_{\ell \in \{m,c,k\}} \left(\tau \, p^{ss*}_T \, q^{\ell f}_{Tt} \right).$$

Real tradable and non-tradable absorption We define absorption as final domestic demand (consumption and investment), netting out intermediate inputs.

We measure real tradable absorption as the quantity of tradable bundles directed specifically toward final domestic demand, valued at their respective steady-state prices p^{ss}_{Tc} and p^{ss}_{Tk}:

$$\text{Real tradable absorption}_t = p^{ss}_{Tc} \, q^c_{Tt} + p^{ss}_{Tk} \, q^k_{Tt}.$$

Similarly, we measure real non-tradable absorption by valuing the non-tradable inputs directed toward final domestic demand at their steady-state price p^{ss}_N:

$$\text{Real non-tradable absorption}_t = p^{ss}_N \, q^c_{Nt} + p^{ss}_N \, q^k_{Nt}.$$

Import prices We compute the Cost, Insurance, and Freight (CIF) import price index as the price of foreign tradable varieties inclusive of both iceberg trade costs and explicit shipping costs h_t:

$$\text{Import price}_t = \tau \, p^*_{Tt} + h_t.$$

Relative prices, Terms of trade, and Real exchange rate To summarize the evolution of the relative price of tradables to non-tradables, we construct a value-weighted average price index of the three tradable bundles (intermediate, consumption, and capital) relative to the non-tradable price p_{Nt}. Let p^ℓ_{Tt} denote the ideal price index of the tradable bundle q^ℓ_{Tt} for sector $\ell \in \{m, c, k\}$. The relative price is defined as:

$$\frac{\tilde{p}_{Tt}}{p_{Nt}} = \frac{\sum_{\ell \in \{m,c,k\}} \omega^\ell_t \, p^\ell_{Tt}}{p_{Nt}},$$

where the time-varying weights represent the value share of each sector's tradable bundle in total domestic tradable expenditure:

$$\omega^\ell_t = \frac{p^\ell_{Tt} \, q^\ell_{Tt}}{\sum_{j \in \{m,c,k\}} p^j_{Tt} \, q^j_{Tt}}.$$

We define the terms of trade as the ratio of the price of imported tradables to the price of exported tradables:

$$\text{Terms of trade}_t = \frac{p^*_{Tt}}{p_{Tt}}.$$

The real exchange rate is defined as the price of the foreign consumption bundle relative to the home consumption bundle. Because the home consumption bundle is our numeraire ($p_t^c \equiv 1$), the real exchange rate simplifies to the price of the foreign consumption bundle:

$$\text{Real exchange rate}_t = \frac{p_t^{c*}}{p_t^c} = p_t^{c*}.$$

7 Estimation

7.1 Structural parameter elasticities

To systematically evaluate how the targeted moments discipline the estimated parameters, we conduct a local sensitivity analysis around the estimated parameter vector $\hat{\theta}$. Let $m(\theta) = \{m_j(\theta)\}_{j=1}^J$ denote the vector of model-implied moments used in estimation. For each estimated parameter θ_i, we perturb the parameter one at a time by a small proportional amount $\Delta_i = \eta\,\hat{\theta}_i$ (where $\eta = 0.01$), holding all other parameters fixed, and summarize the sensitivity of moment m_j to parameter θ_i using elasticities:

$$\mathcal{E}_{j,i} \;\equiv\; \frac{\partial \log m_j(\theta)}{\partial \log \theta_i} \;=\; \frac{\theta_i}{m_j(\theta)}\,\frac{\partial m_j(\theta)}{\partial \theta_i}.$$

We approximate these elasticities numerically at $\hat{\theta}$ using forward finite differences:

$$\widehat{\mathcal{E}}_{j,i} \;\approx\; \frac{\hat{\theta}_i}{m_j(\hat{\theta})} \cdot \frac{m_j(\hat{\theta} + \Delta_i e_i) - m_j(\hat{\theta})}{\Delta_i} \;=\; \frac{m_j(\hat{\theta} + \Delta_i e_i) - m_j(\hat{\theta})}{m_j(\hat{\theta}) \cdot \eta},$$

where e_i is a unit vector that perturbs only parameter θ_i. Larger values of $|\widehat{\mathcal{E}}_{j,i}|$ indicate that variation in moment m_j is more informative about parameter θ_i, providing a transparent mapping between empirical variation and structural parameters.

Table 4 reports the elasticities for the parameters estimated to match business cycle moments. Each row corresponds to a targeted moment and each column to an estimated parameter. The variance of productivity (σ_z^2) is identified almost exclusively by the volatility of real GDP, with an elasticity of 1.00 and negligible sensitivity elsewhere. The capital adjustment cost (Φ_k) is primarily identified by the volatility of investment relative to GDP (elasticity of -0.36), with limited sensitivity to the remaining moments. The import weight (ϕ_τ) is identified by both the volatility of imports relative to tradable output (elasticity of 0.69) and the volatility of investment relative to GDP (elasticity of 0.50). These patterns are consistent with the heuristic identification arguments discussed in the paper.

Table 4: Sensitivity of targeted moments to estimated parameters

	Elasticity w.r.t. parameter (θ_i)		
Targeted moment (m_j)	σ_z^2 (Productivity)	Φ_k (Adj. Cost)	ϕ_τ (Imp. Weight)
Std. dev. Real GDP	1.00	-0.08	0.08
Std. dev. Investment / Std. dev. Real GDP	0.01	-0.36	0.50
Std. dev. Imports / Std. dev. Tradable output	0.02	-0.04	0.69

Each cell reports the elasticity $\mathcal{E}_{j,i} = \frac{\partial \log m_j}{\partial \log \theta_i}$, representing the percentage change in moment m_j in response to a 1% change in parameter θ_i. Values are approximated using forward finite differences around the estimated parameter vector $\hat{\theta}$.

Table 5 reports the elasticities for the parameters estimated to match cross-sectional moments. The weight on domestic capital goods (ζ^k) is primarily identified by the share of capital in aggregate imports (elasticity of -2.54), with additional sensitivity to the share of intermediates in imports and the aggregate import share. The weight on domestic intermediate inputs (ζ^m) exhibits the largest elasticities in the table, and is identified by all three import share moments. The iceberg trade cost (τ) is most sensitive to the aggregate import share (-1.87), as well as the shipping cost import share and relative consumption price. Shipping investment productivity (a_G) is primarily identified by the shipping cost import share (-0.76), with limited sensitivity to the remaining moments. Non-tradable sector productivity (a_N) is almost exclusively identified by the relative consumption price (0.98). Finally, the utilization cost parameter (ϕ) is identified by both the shipping utilization moment (-0.13) and the shipping cost import share (0.17). These patterns are consistent with the heuristic identification discussion in the paper.

Table 5: Sensitivity of cross-sectional moments to estimated parameters

Targeted moment (m_j)	**Elasticity w.r.t. parameter (θ_i)**					
	ζ^k (Cap. weight)	ζ^m (Int. weight)	τ (Iceberg)	a_G (Ship. prod.)	a_N (NT prod.)	ϕ (Util. cost)
Share of agg. imports: Capital	-2.54	4.31	0.60	-0.08	-0.06	0.02
Share of agg. imports: Intermediates	0.58	-3.10	-0.31	0.04	0.02	-0.01
Imports / Absorption	-0.59	-4.47	-1.87	0.18	0.12	-0.04
Shipping costs / Imports	0.05	0.23	-0.73	-0.76	-0.49	0.17
Shipping utilization	0.00	0.00	0.00	-0.13	0.00	-0.13
Relative consumption price (T/NT)	0.00	-0.45	0.52	-0.04	0.98	0.01

Each cell reports the elasticity $\mathcal{E}_{j,i} = \frac{\partial \log m_j}{\partial \log \theta_i}$, representing the percentage change in moment m_j in response to a 1% change in parameter θ_i. Values are approximated using forward finite differences around the estimated parameter vector $\hat{\theta}$.

7.2 Simulation-based standard errors for estimated parameters

Because the estimation relies on moments that are nonlinear functions of time-series data, we compute standard errors for the estimated parameters using a model-based bootstrap.

Let $\hat{\theta}$ denote the vector of parameters estimated from the data using the baseline set of target moments. Starting from $\hat{\theta}$, we repeatedly simulate artificial datasets from the model using the same sample length and stochastic processes as in the data. In each bootstrap replication $b = 1, \ldots, B$, shocks are drawn from the estimated distributions and the model is simulated forward to generate synthetic time series. For each simulated dataset, we construct moments using the same procedures applied to the data, including filtering, detrending, and aggregation. We then re-estimate the model using the same estimation method and target moments, yielding a bootstrap estimate $\hat{\theta}^{(b)}$.

The sampling distribution of the estimator is approximated by the empirical distribution of the bootstrap estimates $\{\hat{\theta}^{(b)}\}_{b=1}^{B}$. Standard errors for each parameter are computed as the sample standard deviation of the bootstrap estimates:

$$\widehat{\mathrm{se}}(\hat{\theta}_i) = \sqrt{\frac{1}{B-1}\sum_{b=1}^{B}\left(\hat{\theta}_i^{(b)} - \bar{\theta}_i\right)^2}, \qquad \bar{\theta}_i = \frac{1}{B}\sum_{b=1}^{B}\hat{\theta}_i^{(b)}.$$

This procedure accounts for finite-sample variation, time-series dependence in the data, and the nonlinear mapping from parameters to moments implied by the model. Table 6 reports bootstrap standard errors and percentile-based confidence intervals for the estimated parameters, together with the distribution of the targeted moments across bootstrap replications.

Table 6: Bootstrap standard errors for estimated parameters and target moments

Parameter	Estimate	S.E.	90% Conf. Int.
σ_z (Prod. shock std.)	0.00325	(0.00039)	[0.00266, 0.00396]
Φ_k (Inv. adj. cost)	0.234	(0.081)	[0.117, 0.396]
ϕ_τ (Imp. weight)	3.547	(0.927)	[2.292, 5.267]

Moment	Data	Mean	S.E.	90% Conf. Int.
Std. dev. Real GDP	1.20	1.20	(0.15)	[0.99, 1.48]
Std. dev. Investment / Std. dev. Real GDP	4.22	4.22	(0.34)	[3.65, 4.77]
Std. dev. Imports / Std. dev. Tradable output	1.35	1.35	(0.22)	[1.03, 1.76]

Note: S.E. denotes bootstrap standard errors. Confidence intervals are based on the 5th and 95th percentiles of the bootstrap distribution across replications.

8 Key Channels and Sensitivity

In this section, we evaluate the sensitivity of our baseline results to a range of alternative specifications. For each specification, we re-estimate the model following the same approach as in the paper. Table 7 reports business cycle statistics and Figures 7 and 8 present results for the COVID-19 exercise. The specifications considered are: (1) the baseline model; (2) a shipping construction lag of 1 period (baseline = 6); (3) a higher shipping cost import share target (baseline $\times$ 2); (4) a shipping industry with market power (baseline = perfect competition); (5) ad-valorem shipping costs (baseline = per-unit); (6) a lower trade elasticity, $\rho = 2$ (baseline = 4); (7) no non-tradable sector; (8) no intermediate inputs; and (9) a first-order model solution (baseline = second-order).

Shipping specifications. Figure 7 reports results for specifications (1)–(5). Shortening the construction lag to one period substantially lowers shipping cost volatility in the business cycle, from 9.84 in the baseline to 5.01, and also narrows the gap in real GDP volatility between the shipping and no-shipping models, from 0.21 in the baseline to 0.11. In the COVID exercise, this specification also implies a smaller contribution of shipping frictions to real GDP dynamics than in the baseline. A higher shipping cost target leaves shipping cost volatility slightly below its baseline value, at 9.29 rather than 9.84, but increases the gap in real GDP volatility between the shipping and no-shipping models, from 0.21 to 0.31. In the COVID exercise, however, it also implies a smaller contribution of shipping frictions to real GDP dynamics than in the baseline. The shipping market power specification leaves the gap in real GDP volatility close to the baseline, while reducing the volatility of shipping costs from 9.84 to 6.24; in the COVID exercise, it also implies a larger role for shipping frictions in shaping real GDP dynamics than in the benchmark case. The ad-valorem specification leaves business-cycle moments close to the baseline and, in the COVID exercise, yields real GDP dynamics very similar to those in the benchmark case.

Technological specifications. Figure 8 reports results for specifications (1) and (6)–(9). Lowering the trade elasticity to $\rho = 2$ raises shipping cost volatility in the business cycle, from 9.84 in the baseline to 13.22, while reducing the gap in real GDP volatility between the shipping and no-shipping models from 0.21 to 0.14. In the COVID exercise, it implies a larger role for shipping frictions in shaping real GDP dynamics than in the baseline. Excluding the non-tradable sector leaves both shipping cost volatility and the gap in real GDP volatility close to their baseline values; in the COVID exercise, it also yields real GDP dynamics that are broadly similar to those in the baseline. Removing intermediate inputs substantially lowers shipping cost volatility, from 9.84 to 6.15, and narrows the gap in real GDP volatility between the shipping and no-shipping models, from 0.21 in the baseline to 0.04. In the COVID exercise, it implies a smaller role for shipping frictions in shaping real GDP dynamics than in the baseline. Finally, using a first-order solution leaves both shipping cost volatility and the gap in real GDP volatility nearly unchanged relative to the baseline, and the COVID dynamics are also very similar.

Table 7: Business cycle fluctuations across model variants

	Model variants																	
	(1) Baseline		(2) Shipping lag=1		(3) Higher shipping cost		(4) Market Power		(5) Ad-valorem		(6) $\rho = 2$		(7) No NT		(8) No IO		(9) 1st order	
	Ship	No Ship	Ship	No Ship	Ship	No Ship	Ship	No Ship	Ship	No Ship	Ship	No Ship	Ship	No Ship	Ship	No Ship	Ship	No Ship
Panel A: Aggregate Production and Trade																		
Std. dev.																		
Real GDP	1.20	1.41	1.20	1.31	1.20	1.51	1.20	1.45	1.20	1.40	1.20	1.34	1.20	1.44	1.20	1.24	1.20	1.41
Net Exports / GDP	0.67	0.64	0.58	0.57	0.81	0.71	0.66	0.58	0.60	0.67	0.59	0.53	0.76	0.72	0.42	0.48	0.67	0.64
Std. dev. relative to real GDP																		
Consumption (c_t)	0.46	0.48	0.32	0.35	0.60	0.75	0.40	0.37	0.43	0.45	0.83	0.97	0.53	0.58	0.31	0.32	0.46	0.49
Investment (i_t)	4.22	4.75	4.22	4.40	4.22	5.22	4.22	4.69	4.22	4.83	4.22	5.18	4.22	4.84	4.14	4.29	4.22	4.78
Labor (n_t)	0.49	0.61	0.52	0.57	0.51	0.66	0.49	0.64	0.50	0.63	0.59	0.61	0.48	0.62	0.54	0.56	0.49	0.61
Panel B: Prices																		
Std. dev. relative to real GDP																		
Tradables–Nontradables price	0.28	0.49	0.23	0.33	0.35	0.78	0.36	0.51	0.28	0.48	0.65	0.90	0.23	0.42	0.24	0.33	0.28	0.50
Terms of trade	1.17	0.98	0.74	0.67	1.83	1.39	0.96	0.75	1.04	0.90	2.04	1.79	1.17	0.96	0.49	0.48	1.19	1.00
Real exchange rate	0.97	0.81	0.53	0.48	1.62	1.22	0.76	0.59	0.84	0.73	1.88	1.64	1.16	0.94	0.53	0.52	0.98	0.82
Panel C: Shipping																		
Std. dev. relative to real GDP																		
Shipping costs (h_t)	9.84	–	5.01	–	9.29	–	6.24	–	10.00	–	13.22	–	9.97	–	6.15	–	9.93	–
Shipping capacity (g_t)	1.03	–	1.21	–	1.11	–	0.84	–	0.99	–	1.35	–	1.05	–	0.53	–	1.05	–
Std. dev.																		
Shipping investment rate ($a_G i_{Gt}/g_t$)	0.67	–	0.84	–	0.64	–	0.60	–	0.67	–	0.83	–	0.65	–	0.52	–	0.68	–

Figure 7: Aggregate dynamics: baseline vs alternative shipping specifications

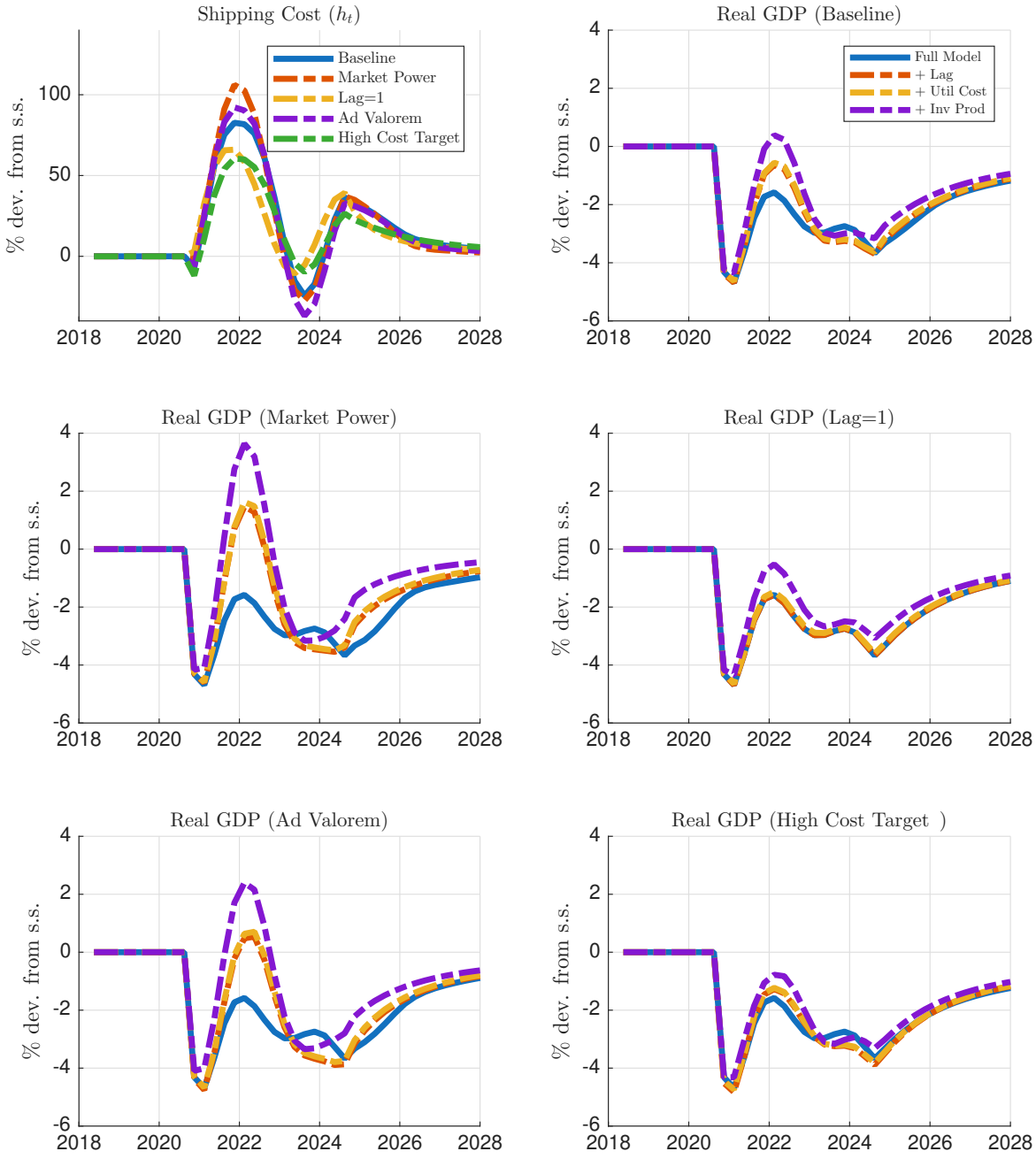

Figure 8: Aggregate dynamics: baseline vs alternative technological specifications

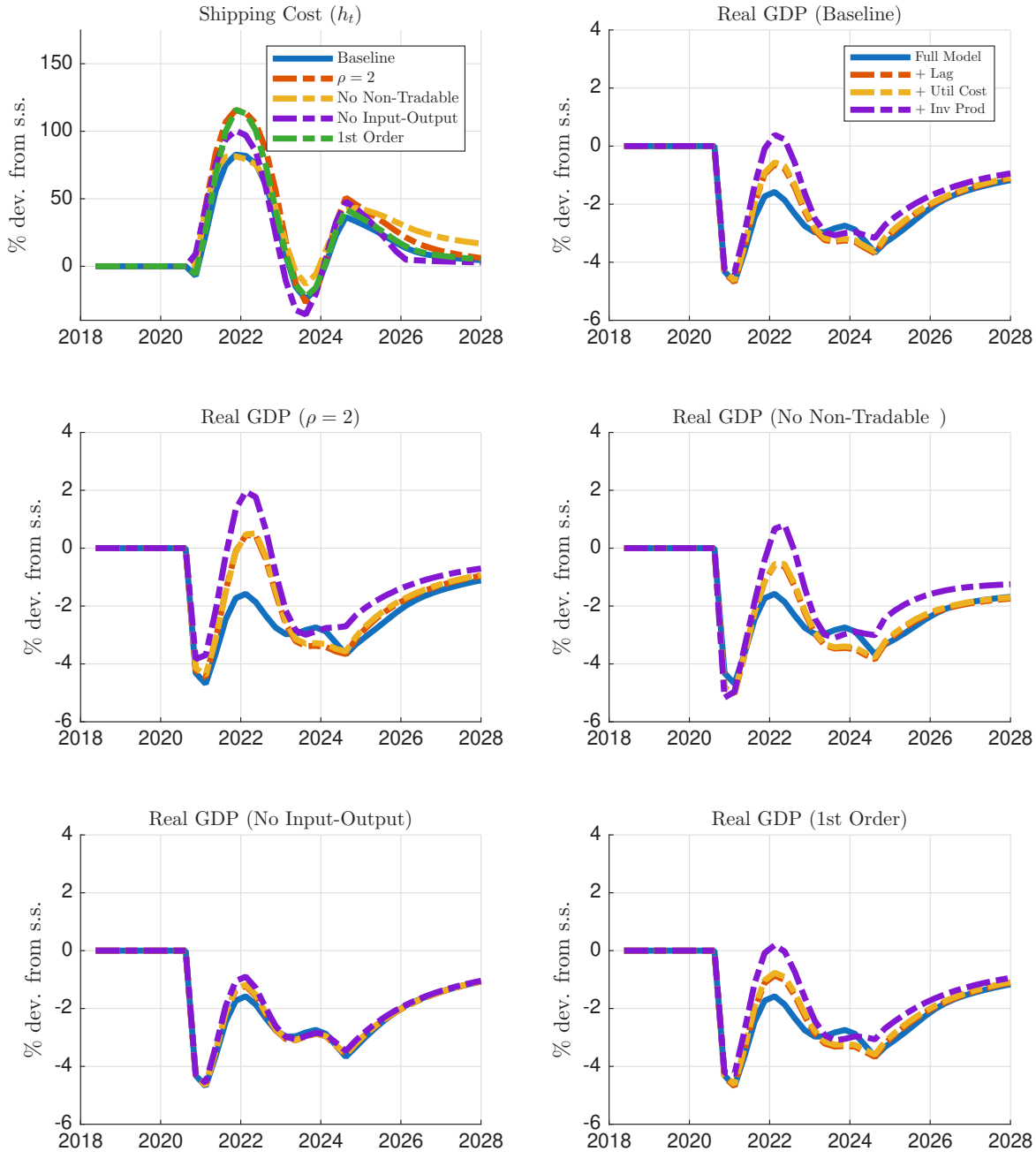

9 Business cycle dynamics

9.1 Correlations with GDP

Table 8 reports the correlations of key variables with real GDP from the baseline model. The shipping model generates lower correlations with real GDP for imports relative to the no-shipping benchmark, consistent with the role of shipping frictions in dampening trade fluctuations. It also yields a more moderate correlation of investment with real GDP, bringing it closer to its empirical counterpart. Some discrepancies relative to the data, particularly for price correlations, are present in both the shipping and no-shipping models and reflect common shortcomings of two-country RBC frameworks.

Table 8: Business cycle correlations with real GDP

	Data	**Shipping**	**No Shipping**
Net Exports / GDP	-0.14	-0.47	-0.40
Consumption (c_t)	0.66	0.94	0.97
Investment (i_t)	0.85	0.85	0.97
Labor (n_t)	0.69	0.96	0.94
Imports	0.82	0.61	0.76
Tradables–Nontradables price	0.16	-0.92	-0.89
Terms of trade	-0.35	0.66	0.57
Real exchange rate	-0.19	0.66	0.57
Shipping costs (h_t)	0.36	0.71	–
Shipping capacity (g_t)	-0.02	-0.13	–
Shipping investment rate ($a_G i_{Gt}/g_t$)	0.26	0.55	–

The table reports correlations with real GDP from the data, the baseline model with endogenous shipping ("Shipping"), and a counterfactual economy with perfectly elastic and costless shipping supply ("No Shipping"). Model moments are computed from HP-filtered logged series (smoothing parameter 1600) and averaged across simulations. Entries marked "–" denote variables that are not defined in the counterfactual economy.

9.2 Transitory shock comparisons

Figures 9 and 10 display impulse responses to a transitory home productivity shock, comparing home against foreign dynamics and the shipping model against the no-shipping benchmark, respectively.

Figure 9 shows that the foreign country's output, consumption, and labor broadly mirror their home counterparts but at a considerably more muted level, as expected given that the shock originates in the home country. Foreign investment exhibits a sharp initial decline on impact while investment rises at home, reflecting a reallocation of resources toward the more productive economy.

Figure 10 illustrates the role of shipping frictions in shaping the transmission of productivity shocks. The shock generates a sharp increase in shipping costs, utilization, and investment in the shipping model, with installed capacity expanding gradually over time as new ships are delivered. Relative to the no-shipping benchmark, the shipping model generates lower import volumes throughout, as shipping frictions raise the cost of trade, while import prices rise more sharply due to the increase in shipping costs. The relative price of tradables falls by less in the shipping model than in the no-shipping benchmark, as rising shipping costs moderate the expansion of tradable exports and limit the decline in tradable prices. The response of output and GDP is broadly similar across the two specifications.

Figure 9: Home v. Foreign Dynamics

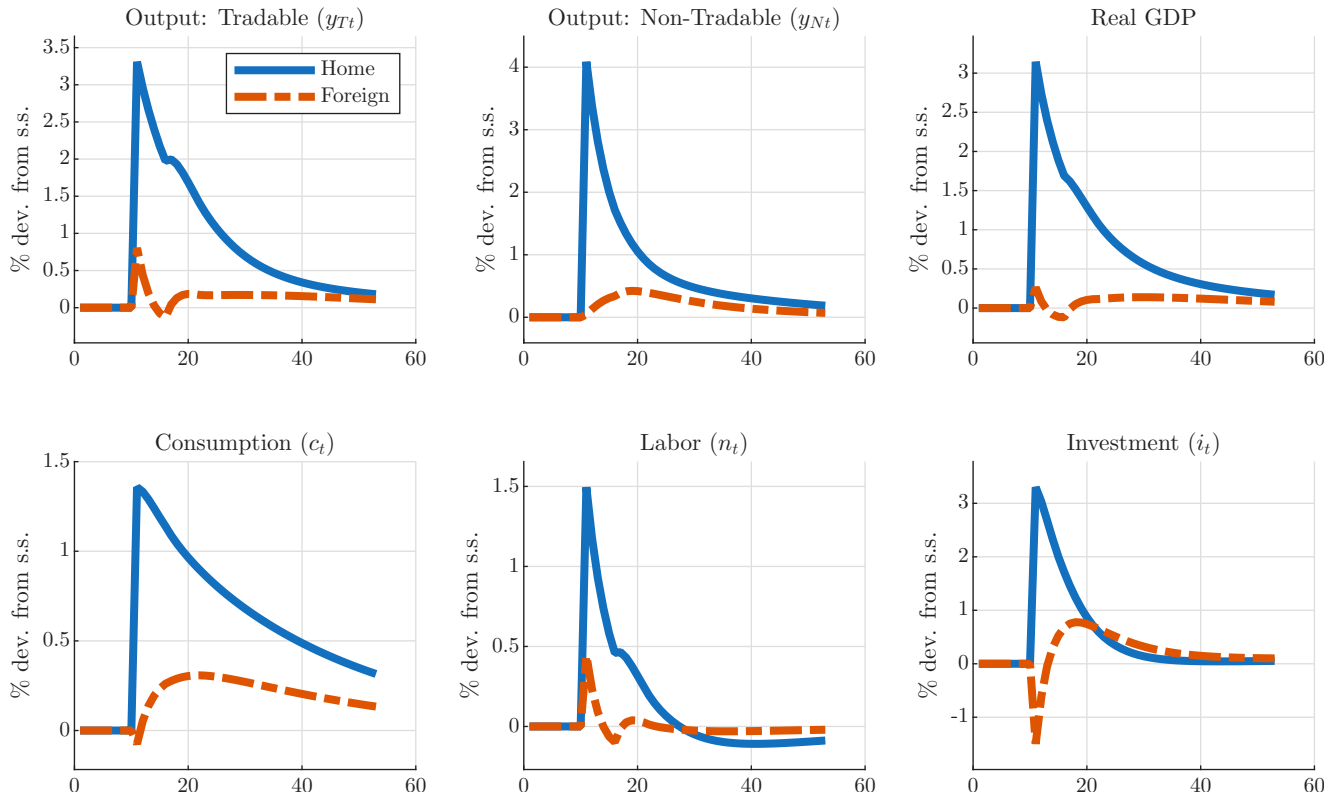

Figure 10: Shipping v. No shipping Dynamics

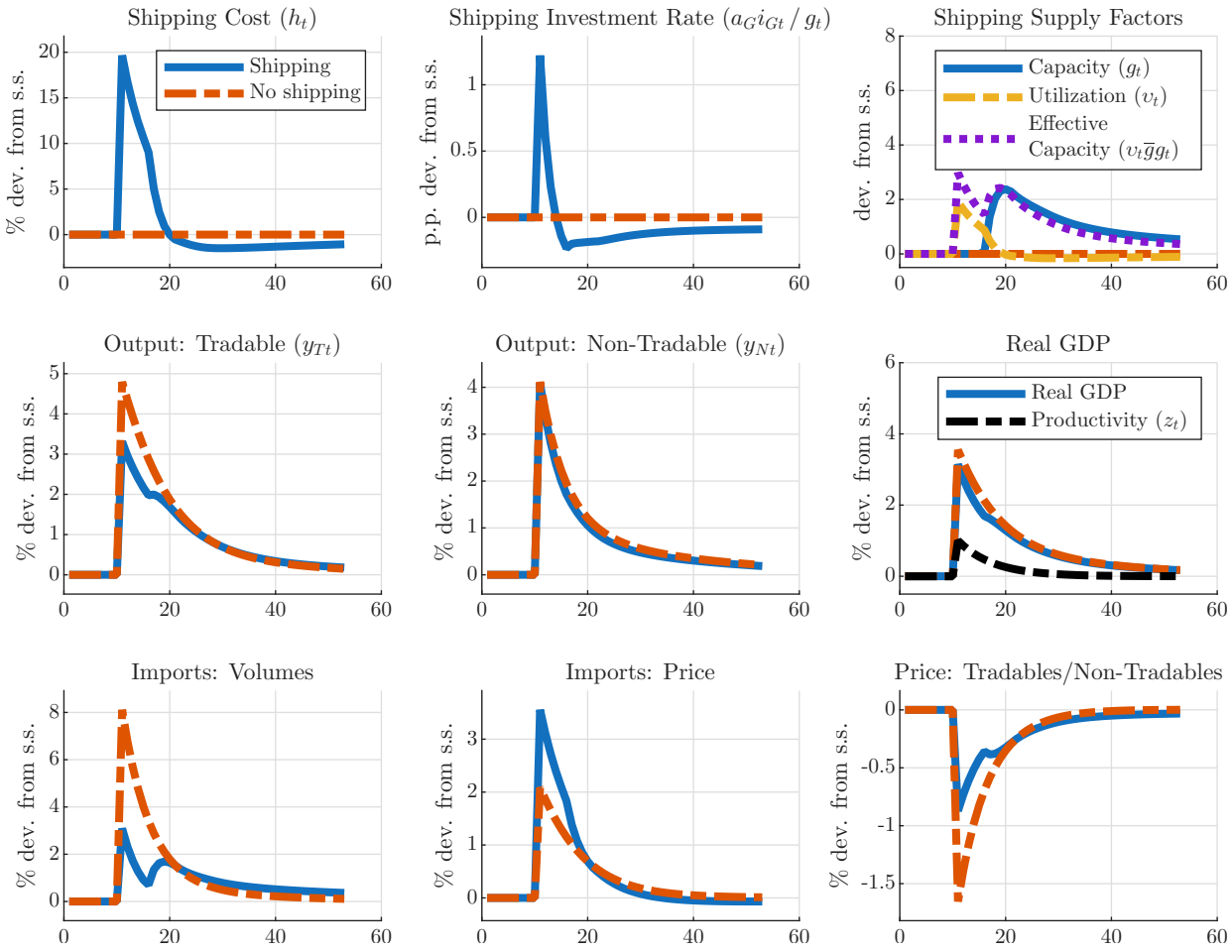

9.3 Local vs. global shocks

Table 9 compares business cycle moments under two shock specifications: the baseline economy, in which home and foreign productivity shocks are uncorrelated, and an alternative in which shocks are perfectly correlated across countries. In the alternative specification, we hold all other parameters fixed at their baseline estimated values, except for the correlation of productivity shocks across countries.

When shocks are perfectly correlated, both countries expand simultaneously, leaving little scope for cross-country reallocation. As a result, the volatility of net exports and international relative prices, including the terms of trade and the real exchange rate, becomes negligible. GDP volatility rises in both the shipping and no-shipping models, but the gap between them widens under correlated shocks, as shipping capacity constraints become more binding when both countries simultaneously place greater demand on shipping services. Consistent with this, the volatility of all shipping variables increases. Notably, investment volatility relative to GDP falls substantially in the shipping model under correlated shocks but remains largely unchanged in the no-shipping benchmark, suggesting that shipping capacity constraints play an important role in dampening investment fluctuations when demand pressures are globally synchronized.

Table 9: Business cycle fluctuations

	Local Shocks		**Global Shocks**	
	Shipping	**No Shipping**	**Shipping**	**No Shipping**
Panel A: Aggregate Production and Trade				
Std. dev.				
Real GDP	1.20	1.41	1.25	1.61
Net Exports / GDP	0.67	0.64	0.07	0.07
Std. dev. relative to real GDP				
Consumption (c_t)	0.46	0.48	0.45	0.49
Investment (i_t)	4.22	4.75	2.95	4.71
Labor (n_t)	0.49	0.61	0.57	0.71
Panel B: Prices				
Std. dev. relative to real GDP				
Tradables–Nontradables price	0.28	0.49	0.35	0.59
Terms of trade	1.17	0.98	0.11	0.09
Real exchange rate	0.97	0.81	0.09	0.07
Panel C: Shipping				
Std. dev. relative to real GDP				
Shipping costs (h_t)	9.84	–	13.15	–
Shipping capacity (g_t)	1.03	–	1.36	–
Std. dev.				
Shipping investment rate ($a_G i_{Gt}/g_t$)	0.67	–	0.93	–

10 Dynamics following COVID-19

10.1 Shipping financial variables

Figure 11 compares untargeted shipping financial variables from the COVID-19 exercise against their empirical counterparts. In the data, we focus on three key financial metrics: the gross profit margin (Gross Profit/Revenue), the EBIT margin (EBIT/Revenue), and stock valuations. These series are constructed from quarterly financial reports and stock prices obtained from Yahoo Finance for a sample of major container shipping firms: Antong, COSCO, Evergreen, Hapag-Lloyd, Korea Line, Maersk, Matson, Swire, and Wan Hai. Financial variables are expressed as log-deviations from the 2015–2019 trend, weighted by total revenue. Stock valuations are measured using firm closing prices adjusted for aggregate market movements by removing the change in the Wilshire 5000 index. In the figures, empirical stock valuations are expressed as log-deviations, while the profit margins are expressed as percentage point deviations from their pre-COVID trend.

To ensure a consistent mapping with these empirical measures, we construct their theoretical counterparts within the model. Revenues are computed as the shipping price h_t times effective shipping supply, and operating expenses correspond to the market value of utilization costs:

$$\text{Revenue}_t = h_t \upsilon_t \, \overline{g} \, g_t,$$

$$\text{Operating expenses}_t = p_{Gt} \, C(\upsilon_t) \, g_t.$$

Gross profit is the difference between revenues and operating expenses:

$$\text{Gross profit}_t = \text{Revenue}_t - \text{Operating expenses}_t.$$

EBIT subtracts depreciation from gross profit. Depreciation is measured at replacement cost p_{Gt}/a_G applied to the depreciated capital stock:

$$\text{Depreciation}_t = p_{Gt} \left(\frac{\delta_G}{a_G} \right) g_{t-1},$$

$$\text{EBIT}_t = \text{Gross profit}_t - \text{Depreciation}_t.$$

Finally, stock valuations V_t are computed as the present discounted value of future shipping profits Θ_t:

$$V_t = \mathbb{E}_t \left[\beta \frac{\Lambda_{t+1}}{\Lambda_t} \left(V_{t+1} + \Theta_{t+1} \right) \right].$$

Consistent with the data, model stock valuations are expressed as log-deviations from their steady state, while the model profit margins are expressed as percentage point deviations.

The model closely matches both the magnitude and dynamics of Gross Profit/Revenue. For EBIT/Revenue, the model captures the general dynamics well but underpredicts the peak. For stock valuations, the model generates a substantial increase but falls short of the peak observed in the data, likely reflecting valuation factors beyond the scope of the model.

Figure 11: COVID-19: Shipping financial variables

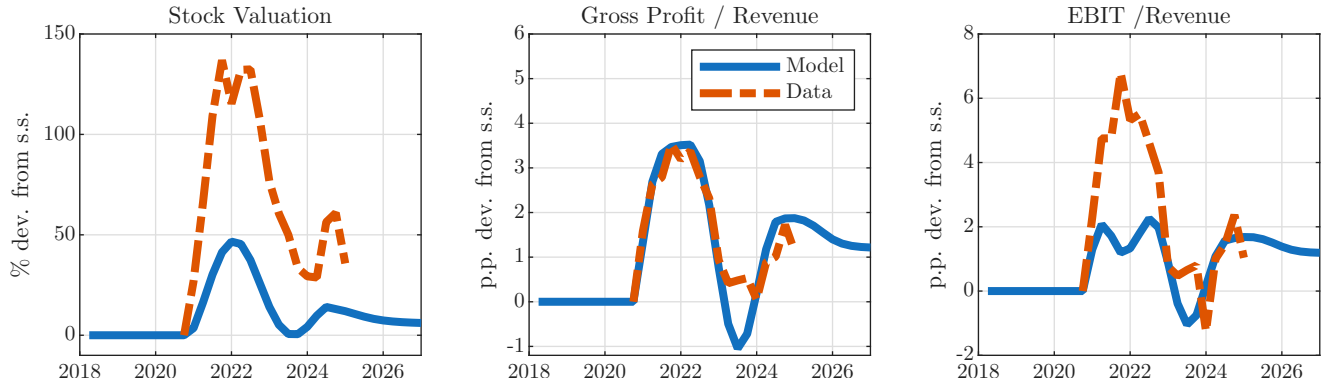

10.2 Identification of COVID shocks

Figure 12 illustrates the identification of the four COVID-era shocks estimated in the paper. To show how each shock is separately identified, we feed each estimated shock into the model one at a time, shutting down the remaining shocks, and compare the implied model dynamics against the estimation targets. We find that each shock has a significant effect on its corresponding target, supporting the identification of the estimated shock processes. Each shock also generates meaningful spillovers to the remaining targets, reflecting the rich propagation mechanisms of the model.

Figure 12: COVID-19: Identification of estimated shocks

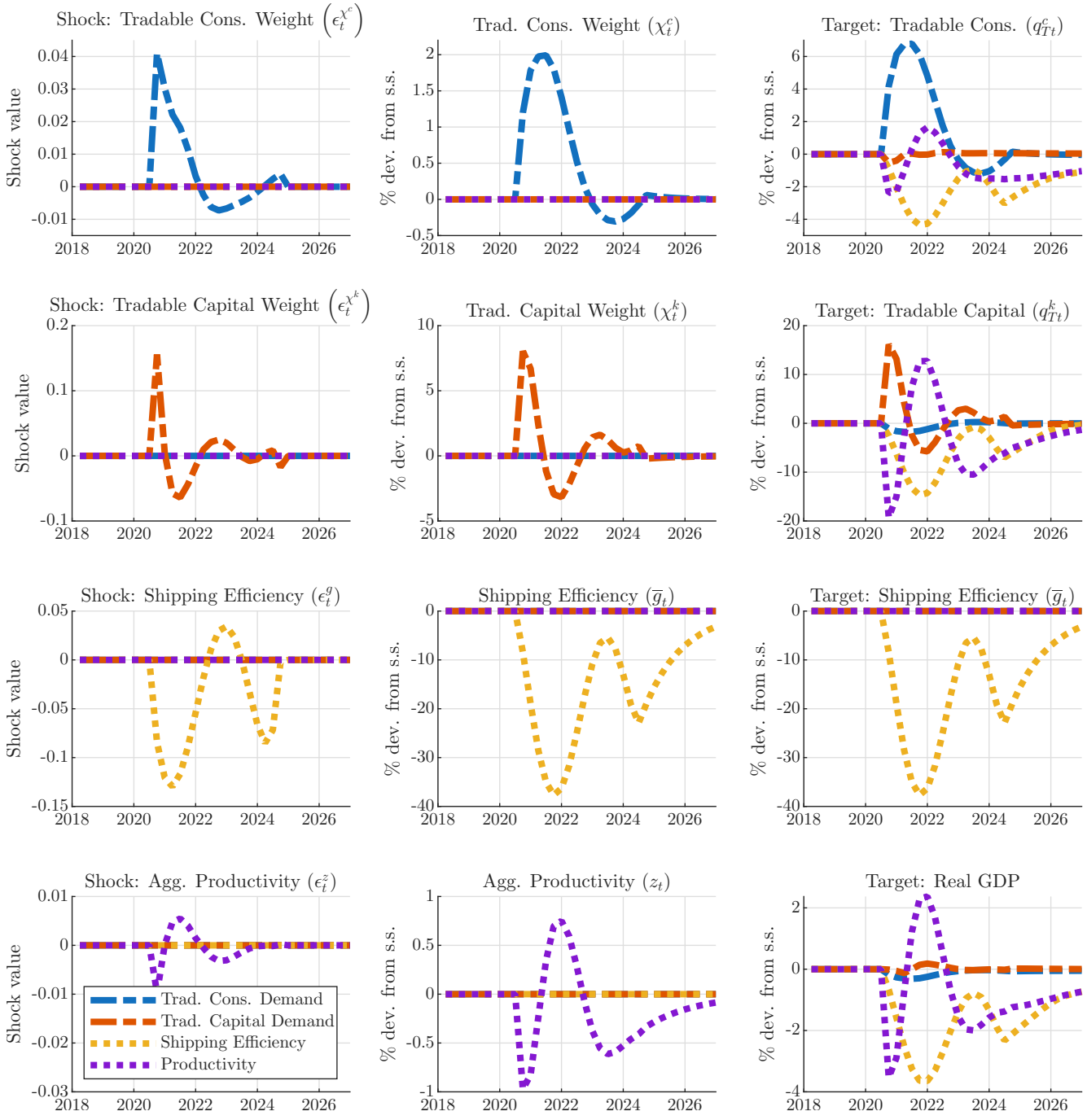

10.3 Alternative shipping efficiency shock target

Figure 13 examines the robustness of the COVID-19 exercise results to the choice of data series used to identify the shipping efficiency shock. The baseline series, reported by Flexport, measures the average trip length across three major routes: China to Northern Europe, China to US East Coast, and China to US West Coast. As an alternative, we consider a series reported by Freightos that measures average ship trip lengths based on transactions in their database, reflecting primarily but not exclusively shipments into the United States.

Re-estimating the shocks under the alternative series yields results that are broadly similar to the baseline, both in terms of the implied path of shipping costs and the role of shipping frictions in accounting for the GDP decline.

Figure 13: COVID-19: Alternative shipping efficiency shock target

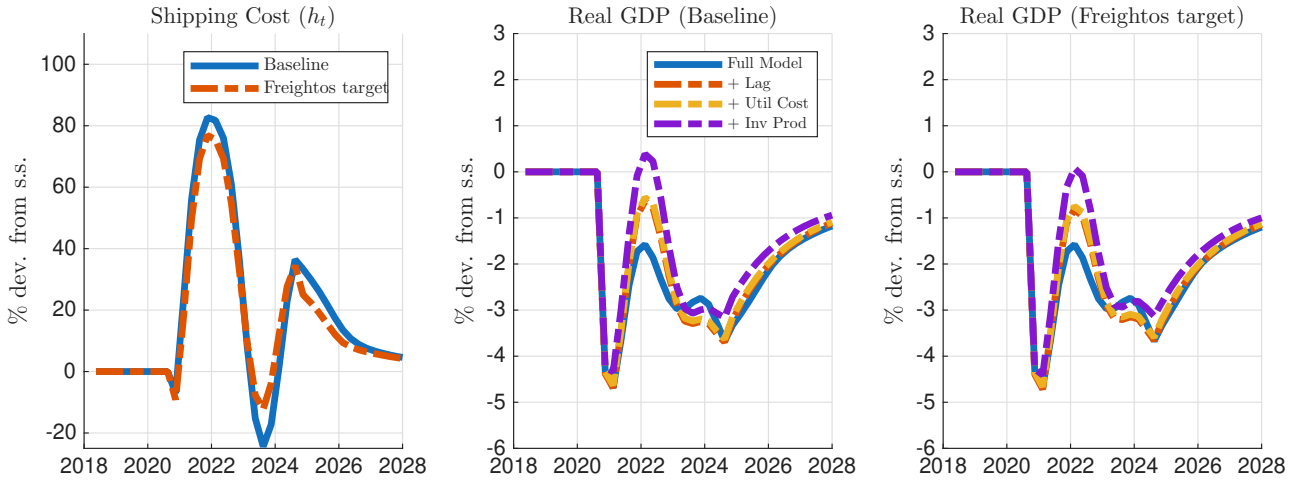

Note: The figure reports results from the COVID-19 exercise under two alternative targets for the shipping efficiency shock: the baseline Flexport series (left and middle panels) and the Freightos series (left and right panels). The middle and right panels decompose the role of shipping in accounting for the GDP decline. The decomposition is cumulative: the dashed orange line adds the shipping production lag ($J = 6$); the dashed yellow line further adds utilization costs; and the dashed purple line further adds shipping investment productivity. All other parameters and shocks are held fixed at their baseline values. Variables are expressed as log deviations from steady state.

11 Model extensions

11.1 Ad-valorem shipping

In the baseline model, international shipments are subject to a per-unit shipping cost h_t, paid per unit of tradable goods shipped internationally. In this extension, we replace per-unit shipping costs with ad-valorem shipping costs that scale proportionally with the value of shipped goods.

Delivered price of imported tradables. Let $s_t \geq 0$ denote the ad-valorem shipping cost. The delivered unit price of an imported tradable variety becomes

$$p_{Tt}^{f,\text{delivered}} = (1 + s_t)\, \tau\, p_{Tt}^*,$$

where τ denotes iceberg trade costs and p_{Tt}^* is the foreign f.o.b. price. Relative to the baseline specification, the additive shipping cost h_t is replaced by the multiplicative factor $(1 + s_t)$.

Accordingly, in the problem of producers of intermediate, consumption, and capital goods, the expenditure on imported tradable varieties is modified as

$$(\tau p_{Tt}^* + h_t)\, q_{Tt}^{\ell f} \quad \rightarrow \quad (1 + s_t)\, \tau p_{Tt}^*\, q_{Tt}^{\ell f}, \qquad \ell \in \{m, c, k\},$$

with all aggregation technologies and demand systems otherwise unchanged.

Shipping capacity constraint. The shipping capacity constraint continues to apply to physical quantities shipped and is unchanged relative to the baseline model:

$$\sum_{\ell \in \{m,c,k\}} \left(q_{Tt}^{\ell f} + q_{Tt}^{\ell h^*} \right) \;\leq\; \upsilon_t\, \overline{g}\, g_t.$$

Global shipping firm. Under ad-valorem shipping, the global shipping firm earns revenues proportional to the value of tradable goods shipped internationally. The value of shipments from the foreign country to the home country equals $\tau p_{Tt}^* \sum_\ell q_{Tt}^{\ell f}$, while the value of shipments from the home country to the foreign country equals $\tau p_{Tt} \sum_\ell q_{Tt}^{\ell h^*}$. Period revenues are therefore given by

$$s_t \left(\tau p_{Tt}^* \sum_{\ell \in \{m,c,k\}} q_{Tt}^{\ell f} + \tau p_{Tt} \sum_{\ell \in \{m,c,k\}} q_{Tt}^{\ell h^*} \right).$$

The global shipping firm chooses shipping investment i_{Gt} and capacity utilization υ_t to maximize the expected discounted sum of profits:

$$\max_{\{g_{t+J},\, \upsilon_t \in [0,1),\, i_{Gt}\}} \mathbb{E}_0 \sum_{t=0}^{\infty} \beta^t \Lambda_t \left\{ s_t \left(\tau p_{Tt}^* \sum_\ell q_{Tt}^{\ell f} + \tau p_{Tt} \sum_\ell q_{Tt}^{\ell h^*} \right) - p_{Gt}\, i_{Gt} - p_{Gt}\, C(\upsilon_t)\, g_t \right\}$$

$$\text{subject to} \quad g_{t+J} = (1 - \delta_G)\, g_{t+J-1} + a_G i_{Gt}, \qquad g_{t+J} \geq 0, \qquad \{g_t\}_{t=0}^{J-1} \text{ given.}$$

As in the baseline model, the shipping market clears when the quantity of tradable goods shipped

internationally equals effective shipping supply,

$$\sum_{\ell \in \{m,c,k\}} \left(q_{Tt}^{\ell f} + q_{Tt}^{\ell h *} \right) \;=\; \upsilon_t \, \overline{g} \, g_t,$$

and the ad-valorem shipping cost s_t adjusts in equilibrium to clear this market.

Ad-valorem revenues and the role of shipping capacity. Under ad-valorem shipping, period revenues equal the ad-valorem rate s_t times the value of international shipments,

$$s_t \left(\tau p_{Tt}^{*} \sum_{\ell} q_{Tt}^{\ell f} + \tau p_{Tt} \sum_{\ell} q_{Tt}^{\ell h *} \right).$$

To make the role of shipping capacity transparent, we can rewrite revenues as

$$s_t \left[\frac{\tau p_{Tt}^{*} \sum_{\ell} q_{Tt}^{\ell f} + \tau p_{Tt} \sum_{\ell} q_{Tt}^{\ell h *}}{\sum_{\ell} \left(q_{Tt}^{\ell f} + q_{Tt}^{\ell h *} \right)} \right] \cdot \sum_{\ell} \left(q_{Tt}^{\ell f} + q_{Tt}^{\ell h *} \right).$$

The term in brackets is the average value per shipped unit (in terms of the model's tradable prices and quantities), while the last term is the total quantity shipped.

When the shipping market clears, revenues can be written as

$$s_t \cdot \bar{p}_t \cdot \upsilon_t \, \overline{g} \, g_t,$$

where $\bar{p}_t$ denotes the average value per shipped unit (the term in brackets above). Thus, conditional on $\bar{p}_t$, the shipping firm's problem consists of choosing investment and utilization taking the effective price of shipping services, $s_t \bar{p}_t$, as given.

11.2 Shipping with market power

In the baseline model, global shipping is modeled as a single firm operating under perfect competition: the shipping price h_t adjusts so that demand for shipping services equals effective shipping supply, and the firm takes this price as given when choosing utilization and investment. In this extension, we relax the assumption of perfect competition and allow for varying degrees of market power in the shipping industry.

We model the global shipping industry as comprising N symmetric firms, indexed by $i \in \{1, \ldots, N\}$. We denote each firm's market share by

$$\kappa \equiv \frac{1}{N},$$

and use this parameter to index the degree of market power: $\kappa = 1$ ($N = 1$) corresponds to a pure monopolist, $\kappa \to 0$ ($N \to \infty$) recovers the competitive baseline, and intermediate values correspond to an oligopolistic market structure. This parameterization allows us to vary the degree of market power while holding the elasticity of substitution across imported varieties fixed.[8]

[8] Under a pure monopolist ($\kappa = 1$), the share of shipping costs in imports is bounded below by a function of the elasticity of substitution across imported varieties ρ. Introducing κ provides the flexibility needed to match the observed shipping cost share without having to change the elasticity of substitution.

Import demand and the shipping price. As in the baseline model, bundle producers $\ell \in \{m, c, k\}$ take the shipping price h_t as given and, as part of their optimization problem, choose imported tradable quantities $q_{Tt}^{\ell f}$ at a delivered unit cost of $\tau p_{Tt}^* + h_t$. Likewise, foreign bundle producers choose $q_{Tt}^{\ell h^*}$ taking the shipping price as given. The resulting demand for shipping services is

$$R_t^D(h_t) \equiv \sum_{\ell \in \{m,c,k\}} \left(q_{Tt}^{\ell f}(h_t) + q_{Tt}^{\ell h^*}(h_t) \right),$$

which is decreasing in h_t. Inverting this schedule, the shipping price consistent with aggregate supply is $h_t = H(R_t)$, where $H(\cdot) \equiv (R_t^D)^{-1}$ and $H'(R_t) < 0$.

Shipping capacity and utilization. Each firm i operates its own shipping fleet with installed capacity $g_{i,t}$ and chooses utilization $\upsilon_{i,t}$. To describe the firm's strategic problem under imperfect competition, we let $\kappa q_{i,t}$ denote firm i's contribution to aggregate shipping supply, subject to the physical feasibility constraint that shipments cannot exceed effective capacity:

$$\kappa q_{i,t} \leq \upsilon_{i,t} \, \overline{g} \, g_{i,t}.$$

In the baseline model, this constraint is implicit because shipping services are determined by market clearing; here, $q_{i,t}$ is an explicit choice that allows the firm to internalize the effect of its supply on the shipping price. Installed capacity evolves according to the same law of motion with time-to-build as in the baseline model, and utilization costs remain given by $C(\upsilon_{i,t})$.

Shipping firms' problem. Let $q_{-i,t}$ denote the supply chosen by a representative rival firm, which firm i takes as given when choosing its own supply $q_{i,t}$. Under symmetry, each of the $N-1$ rival firms supplies $q_{-i,t}$, so rivals collectively account for share $(1-\kappa)$ of aggregate supply, while firm i accounts for share κ. The shipping price faced by firm i is therefore

$$h_t = H(\kappa \, q_{i,t} + (1-\kappa) \, q_{-i,t}),$$

where the firm internalizes the effect of its own choice on h_t through the $\kappa \, q_{i,t}$ term and takes $q_{-i,t}$ as given. Firm i maximizes its profits by choosing $\{g_{i,t+J}, \, \upsilon_{i,t}, \, i_{G,i,t}, \, q_{i,t}\}$:

$$\max_{\{g_{i,t+J},\, \upsilon_{i,t} \in [0,1),\, i_{G,i,t},\, q_{i,t}\}} \mathbb{E}_0 \sum_{t=0}^{\infty} \beta^t \Lambda_t \left\{ H(\kappa \, q_{i,t} + (1-\kappa) \, q_{-i,t}) \, q_{i,t} - p_{Gt} \, i_{G,i,t} - p_{Gt} \, C(\upsilon_{i,t}) \, g_{i,t} \right\}$$

$$\text{subject to} \quad \kappa q_{i,t} \leq \upsilon_{i,t} \, \overline{g} \, g_{i,t},$$

$$g_{i,t+J} = (1-\delta_G) \, g_{i,t+J-1} + a_G i_{G,i,t}, \qquad g_{i,t+J} \geq 0, \qquad \{g_{i,t}\}_{t=0}^{J-1} \text{ given},$$

$$q_{-i,t} \text{ taken as given.}$$

The parameter κ governs the weight of the firm's own supply inside H: a larger κ means the firm's own choice has a larger effect on h_t, generating a larger markup over the shadow marginal cost of capacity.

Equilibrium. All other equilibrium conditions remain unchanged. The equilibrium of the shipping market is symmetric and satisfies $q_{i,t} = q_{-i,t} = R_t$ for all i and t, so the argument of H reduces to aggregate supply R_t. Denoting aggregate capacity, investment, and utilization by $g_t \equiv \sum_i g_{i,t}$, $i_{Gt} \equiv \sum_i i_{G,i,t}$, and $\upsilon_t \equiv \upsilon_{i,t}$ (common across firms), firm-level and aggregate quantities are related by

$$g_{i,t} = \kappa\, g_t, \qquad i_{G,i,t} = \kappa\, i_{Gt}, \qquad \upsilon_{i,t} = \upsilon_t.$$

Summing the firm-level capacity constraint across firms yields the aggregate feasibility condition

$$R_t \;\le\; \upsilon_t\, \overline{g}\, g_t,$$

which binds whenever trade is positive. Similarly, summing the firm-level law of motion for capacity yields the same law of motion for g_t as in the baseline model. The total resource cost of the shipping industry, consisting of utilization costs $p_{Gt}\, C(\upsilon_t)\, g_t$ and investment $p_{Gt}\, i_{Gt}$, takes the same form as in the baseline. The sole modification relative to the baseline is that h_t is pinned down by the shipping firms' optimality conditions rather than by the competitive market-clearing condition, with the dependence on the market structure summarized by κ.

11.3 Shipping utilization microfoundation

This section provides a microfoundation for the shipping capacity utilization specification used in the main model. We first restate the specification employed in the baseline model, and then show how it can be derived from the aggregation of discrete operating decisions across heterogeneous shipping units, in the spirit of Boehm and Pandalai-Nayar (2022).

In the main model, installed shipping capacity g_t is converted into effective shipping services by choosing a utilization rate $\upsilon_t \in [0, 1)$, so that total supply is $S_t = \upsilon_t \bar{g} g_t$, where $\bar{g} > 0$ captures exogenous shipping efficiency. Operating capacity is costly, with utilization costs given by $p_{Gt} C(\upsilon_t) g_t$, where $C(\upsilon) = \phi \left(\frac{\upsilon}{1-\upsilon}\right)^2$ is increasing and convex. Given the shipping price h_t, the firm chooses υ_t taking g_t as given, implying the optimality condition $h_t = \frac{p_{Gt}}{\bar{g}} C'(\upsilon_t)$, which defines an upward-sloping short-run supply curve. We now show how this reduced-form specification can be microfounded from heterogeneous operating decisions across shipping units.

Microfoundation with heterogeneous shipping units. Consider a unit mass of shipping operating units indexed by $i \in [0, 1]$. Each unit represents a ship–route pair or shipping lane and is endowed with a share of aggregate installed capacity, so that total capacity is g_t.

Within period t, each unit makes a discrete operating decision. If unit i operates in period t, it supplies $\bar{g}\, g_t\, di$ units of shipping services; otherwise, it supplies zero. Let $x_{it} \in \{0, 1\}$ denote this operating decision. Aggregate shipping services are therefore

$$S_t = \int_0^1 x_{it}\, \bar{g}\, g_t\, di = \bar{g}\, g_t\, \upsilon_t,$$

where

$$\upsilon_t \equiv \int_0^1 x_{it}\, di \in [0,1]$$

denotes the fraction of operating units that are active. Thus, aggregate utilization υ_t corresponds exactly to the utilization rate in the baseline model.

Heterogeneous operating costs. Operating unit i requires paying a real resource cost proportional to the capacity it controls,

$$\text{Operating cost}_{it} = p_{Gt}\, \kappa_i\, g_t\, di,$$

where $\kappa_i \geq 0$ is an idiosyncratic cost draw capturing heterogeneity across units (e.g., fuel efficiency, congestion exposure, port fees, crew intensity, or repositioning requirements). The distribution of κ_i across units is described by a cumulative distribution function $F(\kappa)$ with corresponding inverse CDF $Q(\upsilon) \equiv F^{-1}(\upsilon)$.

Unit-level decision. Taking the shipping price h_t as given, unit i operates if and only if revenues cover operating costs:

$$x_{it} = 1 \quad \Longleftrightarrow \quad h_t \bar{g} \geq p_{Gt}\, \kappa_i.$$

This implies a cutoff rule. All units with $\kappa_i \leq \kappa_t^\star$ operate, where

$$\kappa_t^\star = \frac{h_t \bar{g}}{p_{Gt}}.$$

As a result, aggregate utilization is

$$\upsilon_t = F(\kappa_t^\star)\,.$$

Aggregation and equivalence. Total operating costs in period t equal

$$\begin{aligned}
\text{Operating cost}_t &= p_{Gt} \int_0^1 \kappa_i\, x_{it}\, g_t\, di \\
&= p_{Gt} g_t \int_{\kappa_i \leq \kappa_t^\star} \kappa_i\, di \\
&= p_{Gt} g_t \int_0^{\upsilon_t} Q(s)\, ds.
\end{aligned}$$

The second line follows from the cutoff rule, which implies that only units with $\kappa_i \leq \kappa_t^\star$ operate. The third line rewrites the integral over operating units in terms of their rank in the cost distribution: since $\upsilon_t = F(\kappa_t^\star)$, the active units correspond to the lowest-cost υ_t fraction of units, and $Q(s) \equiv F^{-1}(s)$ gives the cost of the unit at percentile s. Thus, $\int_0^{\upsilon_t} Q(s)\, ds$ represents the total cost of operating the lowest-cost υ_t fraction of units. Thus, aggregate operating costs take the form $p_{Gt} C(\upsilon_t) g_t$ with

$$C(\upsilon) = \int_0^{\upsilon} Q(s)\, ds.$$

Choosing the distribution of operating costs such that

$$Q(\upsilon) = C'(\upsilon),$$

implies exact equivalence between the aggregate utilization cost in the baseline model and the microfounded aggregation of discrete operating decisions. In particular, for the functional form used in the main model,

$$C(\upsilon) = \phi \left(\frac{\upsilon}{1-\upsilon} \right)^2,$$

differentiation yields

$$C'(\upsilon) = \phi \frac{d}{d\upsilon} \left[\left(\frac{\upsilon}{1-\upsilon} \right)^2 \right] = 2\phi \, \frac{\upsilon}{(1-\upsilon)^3}.$$

Hence, the implied inverse CDF is

$$Q(\upsilon) = 2\phi \, \frac{\upsilon}{(1-\upsilon)^3} = C'(\upsilon).$$

Thus, the cost of activating the marginal operating unit at utilization υ coincides exactly with the marginal aggregate utilization cost in the baseline model. This corresponds to a distribution of operating costs with a steep upper tail, so that increasingly high-cost units must be activated as utilization rises, generating sharply increasing marginal costs.

This microfoundation shows that the utilization cost function employed in the main model can be interpreted as a reduced-form representation of a richer environment in which shipping services are supplied by many heterogeneous operating units making discrete participation decisions. Aggregate convexity arises not from convex costs at the unit level, but from the extensive margin of activating progressively higher-cost units, consistent with the logic emphasized by Boehm and Pandalai-Nayar (2022).

References

Brancaccio, G., M. Kalouptsidi, and T. Papageorgiou (2020): "Geography, transportation, and endogenous trade costs," *Econometrica*, 88, 657–691.

Kalouptsidi, M. (2014): "Time to build and fluctuations in bulk shipping," *American Economic Review*, 104, 564–608.

Kehoe, T. J. and K. J. Ruhl (2008): "Are shocks to the terms of trade shocks to productivity?" *Review of Economic Dynamics*, 11, 804–819.